NETWORKS AND HETEROGENEOUS MEDIA
©American Institute of Mathematical Sciences
Volume **2**, Number **4**, December **2007**

Website: http://aimSciences.org

pp. **661–694**

A CONTINUUM-DISCRETE MODEL FOR SUPPLY CHAINS DYNAMICS

Gabriella Bretti

Istituto per le Applicazioni del Calcolo "M. Picone"
IAC-CNR
Viale del Policlinico, 137
00161 - Rome, Italy

Ciro D'Apice

Dipartimento di Ingegneria dell'Informazione e Matematica Applicata
University of Salerno
Via Ponte Don Melillo
84084 - Fisciano(SA), Italy

Rosanna Manzo

Dipartimento di Ingegneria dell'Informazione e Matematica Applicata
University of Salerno
Via Ponte Don Melillo
84084 - Fisciano(SA), Italy

B. Piccoli

Istituto per le Applicazioni del Calcolo "M. Picone"
IAC-CNR
Viale del Policlinico, 137
00161 - Rome, Italy

Abstract. This paper is focused on continuum-discrete models for supply chains. In particular, we consider the model introduced in [10], where a system of conservation laws describe the evolution of the supply chain status on sub-chains, while at some nodes solutions are determined by Riemann solvers. Fixing the rule of flux maximization, two new Riemann Solvers are defined. We study the equilibria of the resulting dynamics, moreover some numerical experiments on sample supply chains are reported. We provide also a comparison, both of equilibria and experiments, with the model of [15].

1. **Introduction.** Different mathematical approaches have been used to analyse supply chains dynamics. Many of them are based on discrete event simulations and take into account individual parts processed by the supply chain. In the last years continuous models using partial differential equations have been introduced ([1], [2], [10], [20], [15],[17],[18]). We follow the approach used in [10], where the authors proposed a mixed continuum-discrete model and discussed possible choices of solutions at nodes guaranteeing the conservation of fluxes. Starting from the

2000 *Mathematics Subject Classification.* 90B10, 65M06, 65N05.

Key words and phrases. Supply chains, conservation laws, networks, fluid-dynamic models, finite difference schemes.

model in [10], we define two new Riemann Solvers and we introduce discretization algorithms to find approximate solutions to the problems.

A supply chain consists of sequential processors which are going to assemble and construct parts. Each processor is characterized by a maximum processing rate μ_k, its length L_k and the processing time T_k. The rate L_k/T_k represents the processing velocity.

We define a mixed continuum-discrete model in the following way. The supply chain is modelled by a real line seen as a sequence of sub-chains corresponding to intervals I_k such that $I_k \cap I_{k+1} = P_k$: a vertex separating sub-chains. The dynamic of each sub-chain is governed by a continuum system of type

$$\rho_t + f_\varepsilon(\rho, \mu)_x = 0, \tag{1}$$

$$\mu_t - \mu_x = 0, \tag{2}$$

where $\rho(t, x) \in [0, \rho_{max}]$ is the density of objects processed by the supply chain at point x and time t and $\mu(t, x) \in [0, \mu_{max}]$ is the processing rate. For $\varepsilon > 0$, the flux f_ε is given by:

$$f_\varepsilon(\rho, \mu) = \begin{cases} m\,\rho, & \text{if } \rho \le \mu, \\ m\,\mu + \varepsilon(\rho - \mu), & \text{if } \rho \ge \mu, \end{cases} \tag{3}$$

where m is the processing velocity.

We interpret the evolution at nodes P_k thinking to it as Riemann problems for the density equation (1) with μ data as parameters.

Once introduced the model, we discuss possible choices of solutions at nodes P_k guaranteeing the conservation of fluxes for (1). Keeping the analogy to Riemann problems, we call the latter Riemann Solver at nodes. In [10] the authors analysed possible Riemann Solvers fixing the rule:

SC1 The incoming density flux is equal to the outgoing density flux. Then, if a solution with only waves in the density ρ exists, then such solution is taken, otherwise the minimal μ wave is produced.

Rule SC1 corresponds to the case in which processing rate adjustments are done only if necessary, while the density ρ can be regulated more freely. Thus, it is justified in all situations in which processing rate adjustments require re-building of the supply chain, while density adjustments are operated easily (e.g. by stocking). Even if rule SC1 is the most natural also from a geometric point of view, in the space of Riemann data, it produces waves only to lower the value of μ. As a consequence in some cases the value of the processing rate does not increase and it is not possible to maximize the flux.

In order to avoid this problem we analyse two different rules to solve dynamics at a node:

SC2 The objects are processed in order to maximize the flux with the minimal value of the processing rate.

SC3 The objects are processed in order to maximize the flux. Then, if a solution with only waves in the density ρ exists, then such solution is taken, otherwise the minimal μ wave is produced.

According to rule SC2 and SC3 two Riemann Solvers are defined and approximate solutions can be constructed by a wave front tracking algorithm, see [5, 7, 8].

Then we address the problem of numerical simulations for all models. After briefly recalling the Godunov scheme definitions (see also [14]), we use the explicit expressions of the numerical fluxes to implement a *fast* Godunov scheme. The three

different Riemann solvers are tested on examples used in the papers [15, 16]. The latter papers deal with a model, based on a single conservation law, but with the presence of queues in front of each sub-chain. We show how the third Riemann solver SC3 is the more appropriate to reproduce such situation.

The numerical experiments are also useful for a comparison among the three different choices. In particular SC1 appears to be very conservative (as expected), while SC2 and SC3 are more *elastic*, thus allowing more rich dynamics. Then, the main difference between SC2 and SC3 is the following. SC2 tends to make adjustments of the processing rate more than SC3, even when it is not necessary for purpose of flux maximization. Thus, when oscillating waves reach a sub-chain, then SC2 reacts by cutting such oscillations. In conclusion, SC3 is more appropriate to reproduce also the well known "bull-whip" effect, see [9].

The outline of the paper is the following. Section 2 gives the basic definitions of supply chain and Riemann Solver. Then we study the dynamics inside a sub-chain in Section 3, providing flux total variation estimates. In Section 4, general Riemann Solvers at junctions are discussed, then new Riemann Solvers according to rule SC2 and SC3 are defined and explicit unique solutions are given. Section 5 provides analysis of equilibria in a node for Riemann Solvers which respect rule SC1, SC2, and SC3 . In Section 6 we describe Godunov numerical scheme for the system (1)-(2), while in Section 6.1 we construct a simplified version of Godunov scheme for the flux function given by (3). The Riemann Solvers are rewritten for the discretized problems in Section 7. Numerical experiments on sample networks of supply chains are reported and discussed in Section 8, where we establish a comparison with the model proposed in two recent papers [15, 16] by Klar and coauthors and we provide the CPU time used by the simulation algorithm.

2. Basic Definitions.

In this Section we recall basic definitions of the model introduced in [10].

Let us consider a supply chain consisting in a sequence of $N+1$ sub-chains $I_1, \dots, I_{N+1}$, and N vertexes (suppliers) $P_1, ..., P_N$. The supplier P_k connects the sub-chain I_k to the sub-chain I_{k+1}. Each supplier processes a certain good, measured in units of parts, and passes it in the next sub-chain. Each sub-chain I_k is

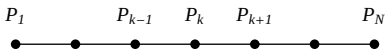

FIGURE 1. A supply chain.

modelled by an interval $[a_k, b_k]$, with P_k corresponding to coordinate b_k, on which we consider the system

$$\begin{cases} \rho_t + f_\varepsilon^k(\rho, \mu)_x = 0, \\ \mu_t - \mu_x = 0. \end{cases} \tag{4}$$

Each sub-chain I_k is thus characterized by a maximum density, a maximum rate and a flux f_ε^k. The flux is defined as in (3), therefore:

(F): $f_\varepsilon^k(\rho,\mu) = \begin{cases} \rho, & 0 \le \rho \le \mu, \\ \mu + \varepsilon(\rho-\mu), & \mu \le \rho \le \rho_k^{\max}, \end{cases}$

or alternatively

$f_\varepsilon^k(\rho,\mu) = \begin{cases} \varepsilon\rho + (1-\varepsilon)\mu, & 0 \le \mu \le \rho, \\ \rho, & \rho \le \mu \le \mu_k^{\max}, \end{cases}$

where $\rho_k^{\max}$ and $\mu_k^{\max}$ are the maximum density and processing rate. From now on, we assume that ε is fixed and, for simplicity, we drop the indexes thus indicate the flux by $f(\rho,\mu)$.

Remark 1. It is possible to generalize all following definitions and results to the case of different fluxes $f_{\varepsilon_k}^k$ for each line I_k (also choosing ε dependent on k). In fact, all statements are in terms of values of fluxes at endpoints of the sub-chains, thus it is sufficient that the ranges of fluxes intersect. Moreover, we can consider different slopes m_k for each line I_k, considering the following flux

$$f_\varepsilon^k(\rho,\mu) = \begin{cases} m_k\rho, & 0 \le \rho \le \mu, \\ m_k\mu + \varepsilon(\rho-\mu), & \mu \le \rho \le \rho_k^{\max}, \end{cases} \tag{5}$$

where $m_k \ge 0$ represents the velocity of each processor and is given by:

$$m_k = \frac{L_k}{T_k},$$

with L_k and T_k, respectively, fixed length and processing time of processor k.

The supply chain evolution is described by a finite set of functions ρ_k, μ_k defined on $[0,+\infty[\times I_k$. On each sub-chain I_k, we say that $U_k := (\rho_k, \mu_k) : [0,+\infty[\times I_k \mapsto \mathbb{R}$ is a weak solution to (4) if, for every C^∞-function $\varphi : [0,+\infty[\times I_k \mapsto \mathbb{R}^2$ with compact support in $]0,+\infty[\times]a_k, b_k[$,

$$\int_0^{+\infty}\int_{a_k}^{b_k} \left(U_k \cdot \frac{\partial\varphi}{\partial t} + f(U_k) \cdot \frac{\partial\varphi}{\partial x} \right) dx\, dt = 0,$$

where

$$f(U_k) = \begin{pmatrix} f(\rho_k,\mu_k) \\ -\mu_k \end{pmatrix},$$

is the flux function of the system (4). For the definition of entropy solution, we refer to [5].

We call Riemann problem for a junction the Cauchy problem corresponding to an initial data which is constant on each supply line.

Definition 2. A Riemann Solver for the supplier P_k consists in a map $RS : [0,\rho_k^{\max}] \times [0,\mu_k^{\max}] \times [0,\rho_{k+1}^{\max}] \times [0,\mu_{k+1}^{\max}] \mapsto [0,\rho_k^{\max}] \times [0,\mu_k^{\max}] \times [0,\rho_{k+1}^{\max}] \times [0,\mu_{k+1}^{\max}]$ that associates to a Riemann data $(\rho_{k,0}, \mu_{k,0}, \rho_{k+1,0}, \mu_{k+1,0})$ at P_k a vector $(\hat\rho_k, \hat\mu_k, \hat\rho_{k+1}, \hat\mu_{k+1})$ so that the solution is given by the waves $(\rho_{k,0}, \hat\rho_k)$ and $(\mu_{k,0}, \hat\mu_k)$ on the sub-chain I_k and by the waves $(\hat\rho_{k+1}, \rho_{k+1,0})$, and $(\hat\mu_{k+1}, \mu_{k+1,0})$ on the sub-chain I_{k+1}. We require the consistency condition

(CC) $RS(RS(\rho_{k,0}, \mu_{k,0}, \rho_{k+1,0}, \mu_{k+1,0})) = RS((\rho_{k,0}, \mu_{k,0}, \rho_{k+1,0}, \mu_{k+1,0}))$.

Once a Riemann Solver is assigned we can define admissible solutions at P_k.

Definition 3. Assume a Riemann Solver RS is assigned for the supplier P_k. Let $U = (U_k, U_{k+1})$ be such that $U_k(t,\cdot)$ and $U_{k+1}(t,\cdot)$ are of bounded variation for

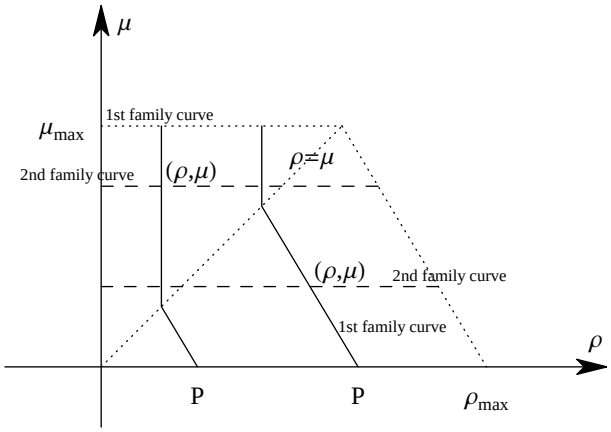

FIGURE 2. First and second family curves

every $t \geq 0$. Then U is an admissible weak solution of (4) related to RS at the junction P_k if and only if the following property holds for almost every t. Setting

$$\widetilde{U}_k(t) = (U_k(\cdot, b_k-), U_{k+1}(\cdot, a_k+))$$

we have $RS(\widetilde{U}_k(t)) = \widetilde{U}_k(t)$.

Our aim is to solve the Cauchy problem on $[0, +\infty[$ for a given initial and boundary data as in next definition.

Definition 4. Given $\bar{U}_k : I_k \mapsto [0,1], k = 1, ..., N$, measurable BV functions, a collection of functions $U = (U_1, ..., U_N)$, with $U_k : [0, +\infty[\times I_k \mapsto [0,1]$ continuous as functions from $[0, +\infty[$ into L^1_{loc} and $U_k(t, \cdot)$ BV function for almost every t, is an admissible solution to the Cauchy problem on the supply chain if U_k is a weak entropy solution to (4) on I_k, $U_k(0, x) = \bar{U}_k(x)$ a.e., and, at each supplier P_k, U is an admissible weak solution.

3. **Dynamics on sub-chains.** Let us fix a sub-chain I_k and analyse system (4): it is a system of conservation laws in the variables $U = (\rho, \mu)$:

$$U_t + F(U)_x = 0, \tag{6}$$

with flux function given by $F(U) = (f(\rho, \mu), -\mu)$. The eigenvectors are given by:

$$r_1(\rho,\mu) = \begin{cases} \begin{pmatrix} 0 \\ 1 \end{pmatrix}, & \text{if } \rho < \mu, \\ \begin{pmatrix} -\frac{1-\varepsilon}{1+\varepsilon} \\ 1 \end{pmatrix}, & \text{if } \rho > \mu, \end{cases} \qquad r_2(\rho,\mu) = \begin{pmatrix} 1 \\ 0 \end{pmatrix}.$$

Hence the Hugoniot curves for the first family are vertical lines above the secant $\rho = \mu$ and lines with slope close to $-1/2$ below the same secant. The Hugoniot curves for the second family are just horizontal lines. Since we consider positive and bounded values for the variables, we fix the invariant region:

$$\mathcal{D} = \{(\rho,\mu) : 0 \leq \rho \leq \rho_{max},\ 0 \leq \mu \leq \mu_{max},$$
$$0 \leq (1+\varepsilon)\rho + (1-\varepsilon)\mu \leq (1+\varepsilon)\rho_{max} = 2(1-\varepsilon)\mu_{max}\}$$

see Figure 2.

Observe that

$$\rho_{\max} = \mu_{\max}\frac{2}{1+\varepsilon}. \tag{7}$$

Lemma 5. *Given an initial datum (ρ_0, μ_0), the maximum value of the density of the curve of the second family passing through (ρ_0, μ_0) and belonging to the invariant region is given by*

$$\rho^M(\mu_0) = \rho_{\max} - \mu_0\frac{\rho_{\max} - \mu_{\max}}{\mu_{\max}}. \tag{8}$$

Proof. From Figure 2, the maximum value is obtained by the intersection of the curve of the second family passing through (ρ_0, μ_0) and the line connecting the points $(\rho_{\max}, 0)$ and $(\mu_{\max}, \mu_{\max})$:

$$\rho^M(\mu_0) = \rho_{\max} - \mu_0\frac{\rho_{\max} - \mu_{\max}}{\mu_{\max}}.$$

From (7) we get

$$\rho^M(\mu_0) = \frac{2}{1+\varepsilon}\mu_{\max} - \frac{1-\varepsilon}{1+\varepsilon}\mu_0. \tag{9}$$

□

The following estimate holds, see [10]:

Proposition 6. *Assume that a second family wave $((\rho_l, \mu_l), (\rho_m, \mu_m))$ interacts with a first family wave $((\rho_m, \mu_m), (\rho_r, \mu_r))$. If $\mu_r < \mu_m$ then the flux variation decreases.*

4. **Riemann Solvers for suppliers for the model (F).** Here, referring to [10], we discuss possible definitions of a general Riemann Solver, which conserves the flux at nodes. We fix a node P_k and a Riemann initial datum: constantly equal to $(\rho_{k,0}, \mu_{k,0})$ on I_k and constantly equal to $(\rho_{k+1,0}, \mu_{k+1,0})$ on I_{k+1}.

Admissible solutions are obtained under the conditions established by the following Lemmas:

Lemma 7. *On the incoming sub-chain, only waves of the first family may be produced, while on the outgoing sub-chain only waves of the second family may be produced.*

Observing that in order to have a solution, the minimum value of incoming flux for the node P_k must be less than the maximum value of the outgoing flux for the node P_k, the following Lemma holds.

Lemma 8. *The Riemann problem at node P_k admits a solution if the following holds: if $\rho_{k,0} \le \mu_{k,0}$ then*

$$\mu_{k+1,0}(1-\varepsilon) + \varepsilon(\rho^M_{k+1} - \frac{2}{1+\varepsilon}\rho_{k,0}) \ge 0. \tag{10}$$

If $\rho_{k,0} > \mu_{k,0}$ then

$$(1-\varepsilon)\left(\mu_{k+1,0} - \frac{\varepsilon}{1+\varepsilon}\mu_{k,0}\right) + \varepsilon(\rho^M_{k+1} - \rho_{k,0}) \ge 0. \tag{11}$$

For the proof of Lemma 8 see [10].

Remark 9. Conditions (10) and (11) are fulfilled if $\rho^M_{k+1} \ge 2\rho_{k,0}$ and $\mu_{k+1,0} \ge \mu_{k,0}$, which is a condition on the initial datum.

From Lemma 7, given the initial datum $(\rho_{k,0}, \mu_{k,0}, \rho_{k+1,0,}, \mu_{k+1,0})$, for every Riemann Solver it follows that

$$\hat{\rho}_k = \varphi(\hat{\mu}_k),$$
$$\hat{\mu}_{k+1} = \mu_{k+1,0},$$

where the function $\varphi(\cdot)$ describes the first family curve through $(\rho_{k,0}, \mu_{k,0})$ as function of $\hat{\mu}_k$. The expression of such curve changes at a particular value $\bar{\mu}_k$, given by:

$$\bar{\mu}_k = \begin{cases} \rho_{k,0}, & \text{if } \rho_{k,0} \le \mu_{k,0}, \\ \frac{1+\varepsilon}{2}\rho_{k,0} + \frac{1-\varepsilon}{2}\mu_{k,0}, & \text{if } \rho_{k,0} > \mu_{k,0}. \end{cases} \tag{12}$$

Let us now discuss how $\hat{\rho}_{k+1}$ and $\hat{\mu}_k$ can be chosen. The conservation of flux at the node can be written as

$$f(\varphi(\hat{\mu}_k), \hat{\mu}_k) = f(\hat{\rho}_{k+1}, \mu_{k+1,0}). \tag{13}$$

We have to distinguish two cases

Case α): $\mu_{k+1,0} < \bar{\mu}_k$;
Case β): $\bar{\mu}_k \le \mu_{k+1,0}$.

In both cases $\bar{\mu}_k$ and $\mu_{k+1,0}$ individuate in the plane $(\hat{\rho}_{k+1}, \hat{\mu}_k)$ four regions, A, B, C, D, so defined:

$$A = \{(\hat{\rho}_{k+1}, \hat{\mu}_k) : 0 \le \hat{\rho}_{k+1} \le \mu_{k+1,0}, \bar{\mu}_k \le \hat{\mu}_k \le \mu_k^{\max}\};$$
$$B = \{(\hat{\rho}_{k+1}, \hat{\mu}_k) : \mu_{k+1,0} \le \hat{\rho}_{k+1} \le \rho_{k+1}^M, \bar{\mu}_k \le \hat{\mu}_k \le \mu_k^{\max}\};$$
$$C = \{(\hat{\rho}_{k+1}, \hat{\mu}_k) : 0 \le \hat{\rho}_{k+1} \le \mu_{k+1,0}, 0 \le \hat{\mu}_k \le \bar{\mu}_k\};$$
$$D = \{(\hat{\rho}_{k+1}, \hat{\mu}_k) : \mu_{k+1,0} \le \hat{\rho}_{k+1} \le \rho_{k+1}^M, 0 \le \hat{\mu}_k \le \bar{\mu}_k\}.$$

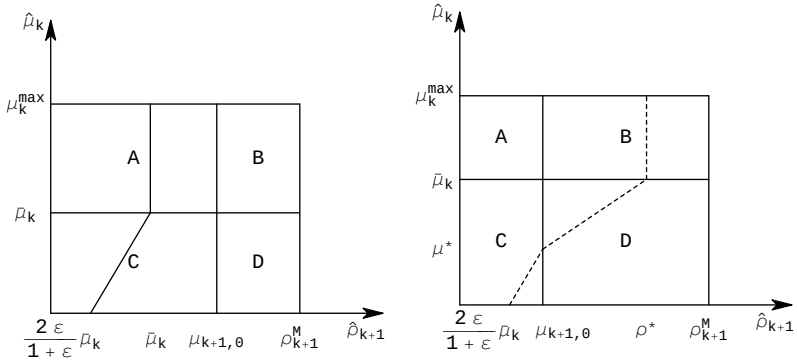

FIGURE 3. Case $\beta) : \bar{\mu}_k \le \mu_{k+1,0}$ and Case $\alpha) : \mu_{k+1,0} < \bar{\mu}_k$.

The equation (13) is satisfied in case β) along the line depicted in Figure 3 and in case α) there are solutions, only under some conditions, along the dashed line. For details we refer the reader to [10].

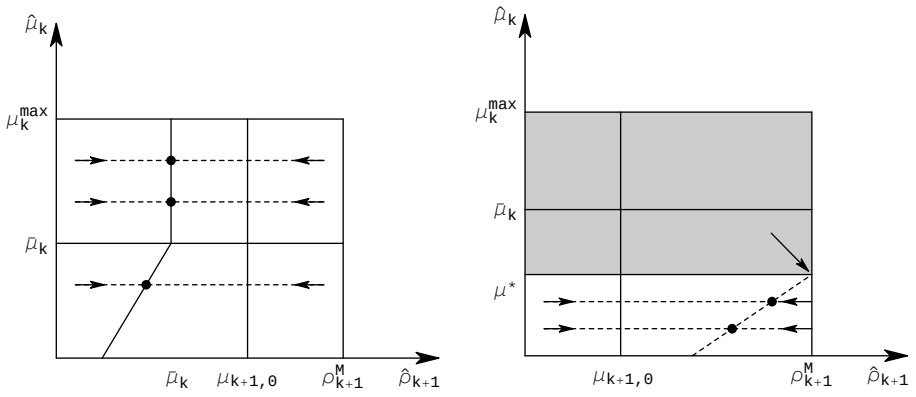

FIGURE 4. An example of Riemann Solver: case β) (on the left) and α) (on the right).

4.1. **A Riemann Solver according to rule SC1.** A geometrically natural Riemann Solver is the following. In case β) we can define a Riemann Solver mapping every initial datum on the line $\hat{\mu}_k = c$ to the intersection of the same line with that drawn in Figure 3.
In case α), it may happen that there is no admissible solution on a given line $\hat{\mu}_k = c$. Therefore, we can use the same procedure if the line $\hat{\mu}_k = c$ intersects the dashed line of Figure 3, while mapping all other points to the admissible solution with the highest value of $\hat{\mu}_k$.

The obtained Riemann Solver is depicted in Figure 4 and satisfies the policy SC1. On the left, there is case β) with all points mapped horizontally, while, on the right, there is case α): all points of the white region are mapped horizontally and all points of the dark region are mapped to the point indicated by the arrow.

Remark 10. If $\hat{\rho}_{k+1} \leq \mu_{k+1,0}$, then the solution $(\hat{\rho}_{k+1}, \rho_{k+1,0})$ is a contact discontinuity. The same happens if $\hat{\rho}_{k+1} \geq \mu_{k+1,0}$ and $\rho_{k+1,0} > \mu_{k+1,0}$. If $\hat{\rho}_{k+1} > \mu_{k+1,0}$ and $\rho_{k+1,0} < \mu_{k+1,0}$, the solution consists of two contact discontinuities.

In the sequel we describe two Riemann Solvers which follow, respectively, rule SC2 and SC3.

4.2. **A Riemann Solver according to rule SC2.** Rule SC2 individuates a specific Riemann Solver:

Theorem 11. *Fix a node P_k. For every Riemann initial datum $(\rho_{k,0}, \mu_{k,0}, \rho_{k+1,0}, \mu_{k+1,0})$ at P_k there exists a unique vector $(\hat{\rho}_k, \hat{\mu}_k, \hat{\rho}_{k+1}, \hat{\mu}_{k+1})$ solution of the Riemann Problem according to rule SC2.*

Proof. Given the initial datum $(\rho_{k,0}, \mu_{k,0}, \rho_{k+1,0,}, \mu_{k+1,0})$, it holds

$$\hat{\rho}_k = \varphi(\hat{\mu}_k),$$
$$\hat{\mu}_{k+1} = \mu_{k+1,0},$$

where $\varphi(\hat{\mu}_k)$ has been defined in the previous section. We have to distinguish again two cases: α) and β).

Case α)**:** $\mu_{k+1,0} < \bar{\mu}_k$. We consider two subcases: $\alpha_1) : \rho^* \leq \rho^M(\mu_{k+1,0})$ and $\alpha_2) : \rho^* > \rho^M(\mu_{k+1,0})$ where

$$\rho^* = \frac{\bar{\mu}_k - (1-\varepsilon)\mu_{k+1,0}}{\varepsilon}. \tag{14}$$

Notice that the two cases correspond to the situation in which solutions in region B exist or do not exist.

: Case α_1). Since $\mu_{k+1,0} < \bar{\mu}_k$ we get

$$\rho^* = \frac{1}{\varepsilon}\bar{\mu}_k - (\frac{1}{\varepsilon} - 1)\mu_{k+1,0} > \frac{1}{\varepsilon}\bar{\mu}_k - (\frac{1}{\varepsilon} - 1)\bar{\mu}_k = \bar{\mu}_k.$$

Consider the lines of Figure 3 (right). To every μ it corresponds a value of the flux. We claim the following:

Claim If $\rho^* \leq \rho^M$ the flux increases with respect to μ along the dashed lines in regions C, D and in B for $\mu_k^{\max} \leq \mu \leq \rho^*$ and, finally, it is constant along the dashed line in region B for $\rho^* \leq \mu \leq \mu_k^{\max}$.

It holds

$$f(\rho^*, \mu) = \begin{cases} \varepsilon\rho^* + (1-\varepsilon)\mu, & 0 \leq \mu \leq \rho^*, \\ \rho^*, & \rho^* \leq \mu \leq \mu_k^{\max}, \end{cases}$$

whose derivative, with respect to μ, is given by

$$\frac{\partial f}{\partial \mu}(\rho^*, \mu) = \begin{cases} (1-\varepsilon), & 0 \leq \mu \leq \rho^*, \\ 0, & \rho^* \leq \mu \leq \mu_k^{\max}. \end{cases}$$

It follows that for $\rho^* \leq \hat{\mu}_k \leq \mu_k^{\max}$ the flux is constant along the dashed line in region B.

Let us now prove that the flux is increasing with respect to μ along the dashed lines in regions C and D. The line connecting the points $(\frac{2\varepsilon}{1+\varepsilon}\bar{\mu}_k, 0)$ and $(\mu_{k+1,0}, \mu^*)$ with $\mu^* = \frac{1+\varepsilon}{1-\varepsilon}(\hat{\mu}_{k+1} - \frac{2\varepsilon}{1+\varepsilon}\bar{\mu}_k)$ has equation

$$\rho - \frac{1}{\mu^*}\left(\mu_{k+1,0} - \frac{2\varepsilon}{1+\varepsilon}\bar{\mu}_k\right)\mu - \frac{2\varepsilon}{1+\varepsilon}\bar{\mu}_k = 0,$$

and a directional vector is given by

$$r_{C_\alpha} = \begin{pmatrix} \frac{1}{\mu^*}\left(\mu_{k+1,0} - \frac{2\varepsilon}{1+\varepsilon}\bar{\mu}_k\right) \\ 1 \end{pmatrix}.$$

Therefore, the directional derivative of the flux is equal to

$$\begin{aligned} \nabla f(\rho, \mu) \cdot r_{C_\alpha} &= \begin{pmatrix} \varepsilon \\ 1-\varepsilon \end{pmatrix} \cdot \begin{pmatrix} \frac{1}{\mu^*}\left(\mu_{k+1,0} - \frac{2\varepsilon}{1+\varepsilon}\bar{\mu}_k\right) \\ 1 \end{pmatrix} \\ &= \frac{\varepsilon}{\mu^*}\left(\mu_{k+1,0} - \frac{2\varepsilon}{1+\varepsilon}\bar{\mu}_k\right) + (1-\varepsilon) > 0. \end{aligned}$$

The latter inequality is fulfilled if $\mu_{k+1,0} > \frac{2\varepsilon}{1+\varepsilon}\bar{\mu}_k$, which is true whenever we have solutions in region C.

In region D a directional vector of the line connecting the points $(\mu_{k+1,0}, \mu^*)$ and $(\rho^*, \bar{\mu}_k)$ is the following

$$r_{D_\alpha} = \begin{pmatrix} \frac{\rho^* - \mu_{k+1,0}}{\bar{\mu}_k - \mu^*} \\ 1 \end{pmatrix}.$$

It implies that

$$\nabla f(\rho,\mu)\cdot r_{D_\alpha} = ([c]c\varepsilon 1-\varepsilon)\cdot\left([c]c\frac{\rho^*-\mu_{k+1,0}}{\bar\mu_k-\mu^*}1\right)$$
$$= \varepsilon\frac{\rho^*-\mu_{k+1,0}}{\bar\mu_k-\mu^*}+(1-\varepsilon)>0,$$

since $\rho^*>\bar\mu_k>\mu_{k+1,0}$ and $\bar\mu_k-\mu^*>0$.

In order to respect rule SC2 we set

$$\hat\rho_{k+1}=\rho^*,$$
$$\hat\mu_k=\min\{\mu_k^{\max},\rho^*\}.$$

: Case α_2). If $\rho^*>\rho^M(\mu_{k+1,0})$, there are not solutions in region B and since the flux increases with respect to μ in region D we set

$$\hat\rho_{k+1}=\rho^M,$$
$$\hat\mu_k=\tilde\mu,$$

where $\tilde\mu$ is obtained from

$$(1-\varepsilon)\mu_{k+1,0}+\varepsilon\hat\rho_{k+1}=(1-\varepsilon)\hat\mu_k+\varepsilon\hat\rho_k,$$

setting $\hat\rho_{k+1}=\rho^M$, i.e.

$$\tilde\mu=\frac{\varepsilon(1+\varepsilon)}{1-\varepsilon}\rho^M-\frac{2\varepsilon}{1-\varepsilon}\bar\mu_k+(1+\varepsilon)\mu_{k+1,0} \tag{15}$$
$$=\frac{2\varepsilon}{1-\varepsilon}(\mu_k^{\max}-\bar\mu_k)+\mu_{k+1,0}.$$

Case β)**:** $\bar\mu_k\le\mu_{k+1,0}$. Consider the line of Figure 3 (left). In this case the flux is constant with respect to μ along the line in the region A and is an increasing function along the line in region C.

In fact, since the line in region A is given by $\hat\rho_{k+1}=\bar\mu_k$, it follows that

$$f(\hat\rho_{k+1},\mu)=\begin{cases}\varepsilon\bar\mu_k+(1-\varepsilon)\mu, & 0\le\mu\le\bar\mu_k,\\ \rho, & \bar\mu_k\le\mu\le\mu_k^{\max},\end{cases}$$

from which

$$\frac{\partial f}{\partial\mu}(\hat\rho_{k+1},\mu)=\begin{cases}(1-\varepsilon), & 0\le\mu\le\bar\mu_k,\\ 0, & \bar\mu_k\le\mu\le\mu_k^{\max}.\end{cases}$$

In region C the line connecting the points $(\frac{2\varepsilon}{1+\varepsilon}\bar\mu_k,0)$ and $(\bar\mu_k,\bar\mu_k)$ has equation

$$\rho-\frac{1-\varepsilon}{1+\varepsilon}\mu-\frac{2\varepsilon}{1+\varepsilon}\bar\mu_k=0,$$

and a directional vector is given by

$$r_{C_\beta}=\begin{pmatrix}\frac{1-\varepsilon}{1+\varepsilon}\\ 1\end{pmatrix}.$$

The directional derivative is the following

$$\nabla f(\rho,\mu)\cdot r_{C_\beta}=\begin{pmatrix}\varepsilon\\ 1-\varepsilon\end{pmatrix}\cdot\begin{pmatrix}\frac{1-\varepsilon}{1+\varepsilon}\\ 1\end{pmatrix}=\varepsilon\frac{1-\varepsilon}{1+\varepsilon}+(1-\varepsilon)>0.$$

It follows that rule SC2 is satisfied if we define

$$\hat\rho_{k+1}=\bar\mu_k,$$
$$\hat\mu_k=\bar\mu_k.$$

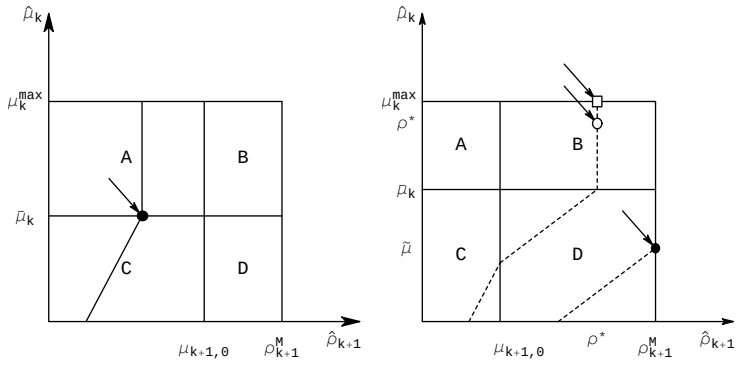

FIGURE 5. Case β) (on the left) and α) (on the right) for the Riemann solver SC2.

Finally the Riemann Solver is the following:

Case α): $\mu_{k+1,0} < \bar{\mu}_k$

Case α_1): $\rho^* \leq \rho^M(\mu_{k+1,0})$

$$\hat{\rho}_{k+1} = \rho^*,$$
$$\hat{\mu}_k = \min\{\mu_k^{\max}, \rho^*\}.$$

Case α_2): $\rho^* > \rho^M(\mu_{k+1,0})$

$$\hat{\rho}_{k+1} = \rho^M(\mu_{k+1,0}),$$
$$\hat{\mu}_k = \tilde{\mu}.$$

Case β): $\mu_{k+1,0} \geq \bar{\mu}_k$

$$\hat{\rho}_{k+1} = \bar{\mu}_k,$$
$$\hat{\mu}_k = \bar{\mu}_k.$$

□

This Riemann Solver is depicted in Figure 5. In case β) we can define a Riemann Solver mapping every initial datum to the point $(\bar{\mu}_k, \bar{\mu}_k)$, indicated by the arrow.

In case α), we can define a Riemann Solver mapping every initial datum to the circle or to the square point if $\rho^* \leq \rho^M$ and to the filled point if $\rho^* > \rho^M$.

4.3. **A Riemann Solver according to rule SC3.** Also rule SC3 permits the determination of a precise Riemann Solver.

Theorem 12. *Fix a node P_k. For every Riemann initial datum $(\rho_{k,0}, \mu_{k,0}, \rho_{k+1,0}, \mu_{k+1,0})$ at P_k there exists a unique vector $(\hat{\rho}_k, \hat{\mu}_k, \hat{\rho}_{k+1}, \hat{\mu}_{k+1})$ solution of the Riemann Problem according to rule SC3.*

Proof. As for the Riemann Solver for rule SC2, given the initial datum $(\rho_{k,0}, \mu_{k,0}, \rho_{k+1,0,}, \mu_{k+1,0})$, we have

$$\hat{\rho}_k = \varphi(\hat{\mu}_k),$$
$$\hat{\mu}_{k+1} = \mu_{k+1,0},$$

The two cases α) and β) are distinguished.

Case α): This case is further split in subcases. First in subcases α_1) and α_2), depending on which among ρ^* and $\rho^M(\mu_{k+1,0})$ is greater.

: Case α_1) : $\rho^* \leq \rho^M(\mu_{k+1,0})$. In Theorem 11 it was proved that the flux increases with respect to μ along the dashed lines in regions C, D and in B for $\mu_k^{\max} \leq \mu \leq \rho^*$ and, finally, it is constant along the line in region B for $\rho^* \leq \mu \leq \mu_k^{\max}$. It follows that we have to consider two possible situations: $\alpha_{1,1}) : \rho^* > \mu_k^{\max}$ and $\alpha_{1,2}) : \rho^* \leq \mu_k^{\max}$.

: Case $\alpha_{1.1}$) : $\rho^* > \mu_k^{\max}$. According to rule SC3 we set

$$\hat{\rho}_{k+1} = \rho^*,$$
$$\hat{\mu}_k = \mu_k^{\max}.$$

: Case $\alpha_{1.2}$) : $\rho^* \leq \mu_k^{\max}$. We set

$$\hat{\rho}_{k+1} = \rho^*,$$
$$\hat{\mu}_k = \max\{\rho^*, \mu_{k,0}\}.$$

: Case α_2) : $\rho^* > \rho^M(\mu_{k+1,0})$. In this case, there are not solutions in region B and since the flux increases with respect to μ in region D we set, as for the Riemann Solver SC2,

$$\hat{\rho}_{k+1} = \rho^M(\mu_{k+1,0}),$$
$$\hat{\mu}_k = \tilde{\mu}.$$

Case β): The flux is constant with respect to μ along the line in the region A and is an increasing function along the line in region C, then we set

$$\hat{\rho}_{k+1} = \bar{\mu}_k,$$
$$\hat{\mu}_k = \begin{cases} \bar{\mu}_k, & \text{if } \mu_{k,0} < \bar{\mu}_k, \\ \mu_{k,0}, & \text{if } \mu_{k,0} \geq \bar{\mu}_k. \end{cases}$$

□

The obtained Riemann Solver is depicted in Figure 6: all points of the white region are mapped horizontally and all points of the dark regions are mapped to the point indicated by the arrows.

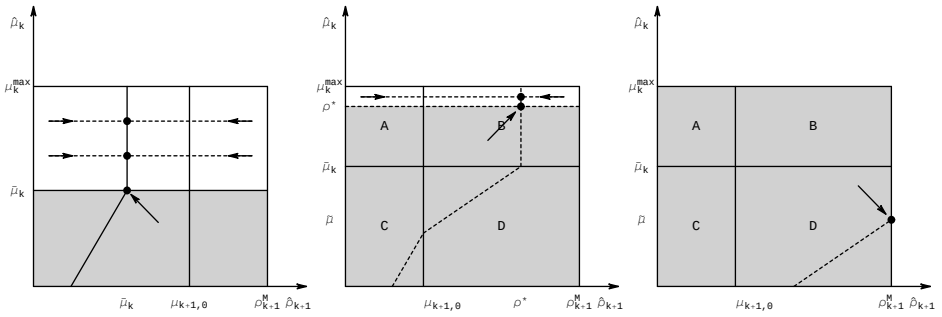

FIGURE 6. Case β) and α) (namely α_1) and α_2)) for the Riemann Solver SC3.

In the following lemma we consider solvability of Riemann Problems according to the Riemann Solvers presented.

Lemma 13. *Consider a supply chain on which the initial datum verifies* $\mu_{k,0} = \mu_k^{max}$*, i.e. the production rate is at its maximum. A sufficient condition for the solvability of all Riemann problems, according to rule SC2 or SC3, on the supply chain at every time is*

$$\rho_{k+2}^{\max} \geq \rho_k^{\max}, \forall k.$$

The proof is similar to the corresponding Lemma of [10].

5. **Analysis of equilibria.** In this section we discuss the equilibria at nodes. We fix a node P_k and a Riemann initial datum $\rho_0 = (\rho_{k,0}, \mu_{k,0}, \rho_{k+1,0}, \mu_{k+1,0})$.

Definition 14. Define $\hat{\rho} = RS(\rho_0)$. The datum ρ_0 is an equilibrium if

$$\hat{\rho} = RS(\rho_0) = \rho_0.$$

The conservation of flux at the node can be written as

$$f(\rho_{k,0}, \mu_{k,0}) = f(\rho_{k+1,0}, \mu_{k+1,0}),$$

and it is satisfied in accordance to the Riemann Solvers. From now on, we suppose that the sub-chains have the same maximum processing rate, i.e $\mu_k^{\max} = \mu_{k+1}^{\max}, \forall k$.

5.1. **Riemann Solver SC1.** Let us analyse the case $\alpha)$: $\mu_{k+1,0} < \bar{\mu}_k$ and $\beta)$: $\mu_{k+1,0} \geq \bar{\mu}_k$.

Case α)**:** We have to discuss the subcases $\alpha_1)$: $\rho^* \leq \rho^M(\mu_{k+1,0})$ and $\alpha_2)$: $\rho^* > \rho^M(\mu_{k+1,0})$.

Case α_1)**:** In this case $\mu_{k,0}, \rho_{k,0}$ and $\mu_{k+1,0}$ can assume all positive values, with $\mu_{k+1,0}$ subject to the constraint $\mu_{k+1,0} < \bar{\mu}_k = \bar{\mu}_k(\rho_{k,0}, \mu_{k,0})$, while $\rho_{k+1,0} = \rho_{k+1,0}(\rho_{k,0}, \mu_{k+1,0})$.

Case α_2)**:** We have $\mu_{k,0} \leq \tilde{\mu}(\rho_{k,0}, \mu_{k+1,0})$. Since $\mu_{k,0} < \bar{\mu}_k$, it follows that $\rho_{k,0} \geq \mu_{k,0}$ from which we obtain $\bar{\mu}_k = \mu_{k,0} + \varepsilon(\rho_{k,0} - \mu_{k,0})$. Finally, we have that $\rho_{k,0}$ $\mu_{k,0}$ and $\mu_{k+1,0}$ can assume all the positive values, with $\mu_{k+1,0}$ subject to the conditions $\mu_{k+1,0} \leq \mu_{k,0} + \varepsilon(\rho_{k,0} - \mu_{k,0}), \mu_{k,0} \leq \tilde{\mu}(\rho_{k,0}, \mu_{k+1,0})$ and $\rho_{k+1,0} = \rho_{k+1,0}(\rho_{k,0}, \mu_{k+1,0})$.

Case β)**:** In this case $\rho_{k,0}$ $\mu_{k,0}$ and $\mu_{k+1,0}$ can assume all positive values, with $\mu_{k+1,0}$ subject to the constraint $\mu_{k+1,0} \geq \bar{\mu}_k$ and $\rho_{k+1,0} = \rho_{k+1,0}(\rho_{k,0}, \mu_{k+1,0})$.

5.2. **Riemann Solver SC2.** Let us distinguish the case $\alpha)$ and $\beta)$.

Case α)**:** We have to consider the subcases $\alpha_1)$: $\rho^* < \rho^M(\mu_{k+1,0})$ and $\alpha_2)$: $\rho^* \geq \rho^M(\mu_{k+1,0})$. Let us start considering case $\alpha_1)$.

Case α_1)**:** In this case, from the Riemann Solver we get

$$\begin{aligned} \rho_{k+1,0} &= \rho^* > \bar{\mu}_k, \\ \mu_{k,0} &= \min\{\mu_k^{\max}, \rho^*\} \leq \rho_{k+1,0}, \\ \mu_{k,0} &\geq \bar{\mu}_k. \end{aligned}$$

From the latter inequality, using (12), it follows that $\bar{\mu}_k = \rho_{k,0}$. The hypothesis $\mu_{k+1,0} < \bar{\mu}_k$ implies that

$$\mu_{k+1,0} < \bar{\mu}_k = \rho_{k,0} \leq \mu_{k,0} \leq \rho_{k+1,0}. \tag{16}$$

Moreover, the relation $\rho^* < \rho^M(\mu_{k+1,0})$ leads to

$$\rho_{k,0} < \frac{2\varepsilon}{1+\varepsilon}\mu_k^{\max} + \frac{1-\varepsilon}{1+\varepsilon}\mu_{k+1,0}. \tag{17}$$

Remark 15. If $\varepsilon = 0$, from (17) we get $\rho_{k,0} < \mu_{k+1,0}$, relation that is in contradiction with (16). In fact in this case ρ^* is not defined. It follows that there are not equilibria for $\varepsilon = 0$.

Since $\mu_{k,0} = \min\{\mu_k^{\max}, \rho^*\}$, consider now two cases $\alpha_{1.1}) : \mu_k^{\max} \leq \rho^*$ and $\alpha_{1.2}) : \mu_k^{\max} > \rho^*$.

Case $\alpha_{1.1}$): In this case we have

$$\begin{aligned} \mu_{k,0} &= \mu_k^{\max}, \\ \rho_{k+1,0} &\geq \mu_k^{\max}. \end{aligned} \tag{18}$$

Taking into account that $\rho_{k+1} = \rho^*$ and using (14) and (17) we get

$$\mu_k^{\max} \leq \rho_{k+1,0} < \frac{2}{1+\varepsilon}\mu_k^{\max} - \frac{1-\varepsilon}{1+\varepsilon}\mu_{k+1,0} = \rho^M(\mu_{k+1,0}). \tag{19}$$

Starting from a fixed value of $\rho_{k,0}$, we discuss the equilibria. Since (17) holds supposing that $\rho_{k,0}$ assumes the maximum value

$$\frac{2\varepsilon}{1+\varepsilon}\mu_k^{\max} + \frac{1-\varepsilon}{1+\varepsilon}\mu_{k+1,0},$$

we get the following value for $\mu_{k+1,0}$

$$\mu_1(\rho_{k,0}) = \frac{1+\varepsilon}{1-\varepsilon}\rho_{k,0} - \frac{2\varepsilon}{1-\varepsilon}\mu_k^{\max}. \tag{20}$$

From (16) and (18) it follows that if $\rho_{k,0} \in [0, \mu_k^{\max}]$, then $\mu_{k+1,0} \in [\mu_1, \rho_{k,0}]$. The relation (19) implies that the maximum value $\rho_{k+1,0}$ can assume is given by

$$\rho_{k+1,0} = \rho_{k+1,0}(\rho_{k,0}, \mu_{k+1,0}) = \frac{2\varepsilon}{1+\varepsilon}\mu_k^{\max} - \frac{1-\varepsilon}{1+\varepsilon}\mu_{k+1,0},$$

that is a decreasing function with respect to $\mu_{k+1,0}$.

Using (20) we can express $\rho_{k+1,0}$ in function of $\rho_{k,0}$ and $\mu_k^{\max}$

$$\rho_{k+1,0} = \rho^* = 2\mu_k^{\max} - \rho_{k,0},$$

therefore $\rho_{k+1,0} \in [\mu_k^{\max}, 2\mu_k^{\max} - \rho_{k,0}]$. Since $\rho_{k+1,0} \geq \mu_k^{\max}$, it follows that $\mu_{k+1,0} \in [\mu_1(\rho_{k,0}), \mu_2(\rho_{k,0})]$ where

$$\mu_2(\rho_{k,0}) = \frac{1}{1-\varepsilon}\rho_{k,0} - \frac{\varepsilon}{1-\varepsilon}\mu_k^{\max}.$$

It remains to establish the conditions ensuring that $\mu_2(\rho_{k,0}) \geq 0$ and $\mu_2(\rho_{k,0}) \leq \mu_k^{\max}$. The second relation is always fulfilled since $\rho_{k,0} \leq \mu_{k,0}$. Instead, the first holds if

$$\rho_{k,0} \geq \varepsilon\mu_{k,0} = \varepsilon\mu_k^{\max}. \tag{21}$$

Remark 16. Notice that if $\rho_{k,0} = \varepsilon\mu_{k,0}$ we have $\mu_{k+1,0} = 0$ and $\rho_{k+1,0} = \mu_k^{\max}$.

If (20) is satisfied the equilibria configurations depend on the value of $\mu_1(\rho_{k,0})$. We have that $\mu_1(\rho_{k,0}) \gtreqless 0$ if $\rho_{k,0} \gtreqless \frac{2\varepsilon}{1+\varepsilon}\mu_k^{\max}$. In the case $\mu_1(\rho_{k,0}) < 0$, since $\mu_{k+1,0} = 0$ implies that $\rho_{k+1,0} = \frac{\rho_{k,0}}{\varepsilon}$, we obtain that $\rho_{k+1,0} \in [\mu_k^{\max}, \frac{\rho_{k,0}}{\varepsilon}]$.

Finally, the set of equilibria is defined in the following way: $\mu_{k,0} = \mu_k^{\max}$, $\rho_{k,0} \in [\varepsilon\mu_k^{\max}, \mu_k^{\max}]$. In particular, we have to consider two cases:

Case $\alpha_{1.1.1}$): If $\rho_{k,0} \in [\varepsilon\mu_k^{\max}, \frac{2\varepsilon}{1+\varepsilon}\mu_k^{\max}]$, then we have $\mu_{k+1,0} \in [0, \mu_2(\rho_{k,0})]$, $\rho_{k+1,0} = \rho^*(\rho_{k,0}, \mu_{k+1,0}) \in [\mu_k^{\max}, \frac{\rho_{k,0}}{\varepsilon}]$.

Case $\alpha_{1.1.2}$)**:** If $\rho_{k,0} \in [\frac{2\varepsilon}{1+\varepsilon}\mu_k^{\max}, \mu_k^{\max}]$, then we have $\mu_{k+1,0} \in [\mu_1(\rho_{k,0}), \mu_2(\rho_{k,0})]$, $\rho_{k+1,0} = \rho^*(\rho_{k,0}, \mu_{k+1,0}) \in [\mu_k^{\max}, \rho^M(\mu_{k+1,0})]$.

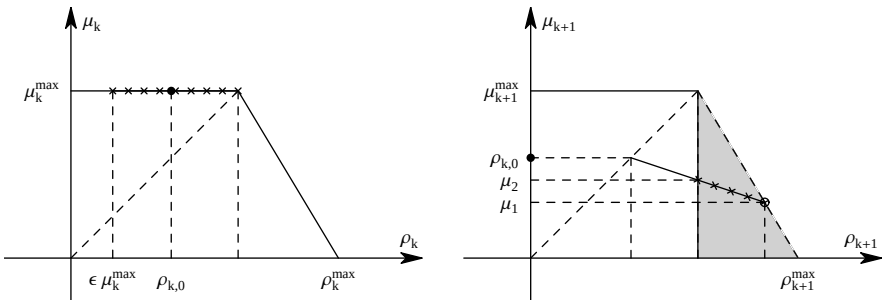

FIGURE 7. Equilibria configurations for the Case $\alpha_{1.1}$).

Equilibria configurations are depicted in Figure 7. Observe that fixed $\rho_{k,0}$ we have a segment on the outgoing sub-chain. If $\rho_{k,0}$ varies in the interval $[\varepsilon\mu_k^{\max}, \mu_k^{\max}]$, we get a region on the outgoing sub-chain, coloured in grey, without the oblique side. Moreover, the processing rate is maximum on the incoming sub-chain and assumes values in $[\mu_1(\rho_{k,0}), \mu_2(\rho_{k,0})]$ on the incoming one, while the density on the outgoing sub-chain is greater than the density on the incoming one.

Case $\alpha_{1.2}$)**:** From $\mu_k^{\max} > \rho^*$ it follows that $\rho_{k+1,0} = \mu_{k,0} = \rho^*$. Finally we have

$$\mu_{k+1,0} < \rho_{k,0} \leq \rho_{k+1,0} = \rho^*(\rho_{k,0}, \mu_{k+1,0}) < \mu_k^{\max}.$$

In this case $\rho^* = \rho_{k+1,0} \in [\rho_{k,0}, \mu_k^{\max}]$, in fact if $\mu_{k+1,0} = \rho_{k,0}$ we have $\rho^* = \rho_{k,0}$. From the Case $\alpha_{1.1}$) we get $\rho_{k,0} \in [\varepsilon\mu_k^{\max}, \mu_k^{\max}]$. We have to distinguish two cases:

Case $\alpha_{1.2.1}$)**:** If $\rho_{k,0} \in [0, \varepsilon\mu_k^{\max}]$, then we have $\mu_{k+1,0} \in [0, \rho_{k,0}]$, $\rho_{k+1,0} = \rho^*(\rho_{k,0}, \mu_{k+1,0}) = \mu_{k,0} \in [\rho_{k,0}, \frac{\rho_{k,0}}{\varepsilon}]$.

Case $\alpha_{1.2.2}$)**:** If $\rho_{k,0} \in [\varepsilon\mu_k^{\max}, \mu_k^{\max}]$, then we have $\mu_{k+1,0} \in [\mu_2(\rho_{k,0}), \rho_{k,0}]$, $\rho_{k+1,0} = \rho^*(\rho_{k,0}, \mu_{k+1,0}) = \mu_{k,0} \in [\rho_{k,0}, \mu_k^{\max}]$.

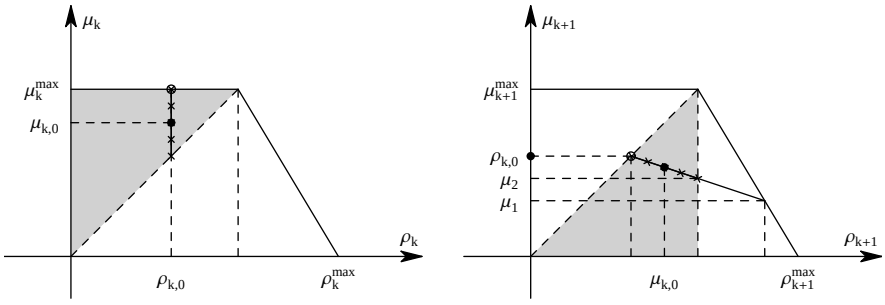

FIGURE 8. Equilibria configurations for the Case $\alpha_{1.2}$).

Equilibria configurations are depicted in Figure 8. Observe that at a point on the incoming sub-chain corresponds a point on the outgoing sub-chain.

Moreover, the density on the outgoing sub-chain is equal to the processing rate on the incoming sub-chain.

Case α_2): In this case $\mu_{k+1,0} < \bar{\mu}_k$. According to the Riemann Solver

$$\mu_{k,0} = \tilde{\mu} = \frac{2\varepsilon}{1-\varepsilon}(\mu_k^{\max} - \bar{\mu}_k) + \mu_{k+1,0}. \tag{22}$$

Since $\mu_{k,0} = \tilde{\mu} \leq \bar{\mu}_k$, from the definition of $\bar{\mu}_k$ it follows that

$$\bar{\mu}_k = \frac{1+\varepsilon}{2}\rho_{k,0} + \frac{1-\varepsilon}{2}\mu_{k,0}, \tag{23}$$

and $\rho_{k,0} \geq \mu_{k,0}$. Using (23), the relation (22) reads

$$\mu_{k,0} = \frac{2\varepsilon}{1-\varepsilon^2}\mu_k^{\max} - \frac{\varepsilon}{1-\varepsilon}\rho_{k,0} + \frac{1}{1+\varepsilon}\mu_{k+1,0}. \tag{24}$$

Finally, we have

$$\begin{aligned} \rho_{k,0} \geq \mu_{k,0} &= \frac{2\varepsilon}{1-\varepsilon^2}\mu_k^{\max} - \frac{\varepsilon}{1-\varepsilon}\rho_{k,0} + \frac{1}{1+\varepsilon}\mu_{k+1,0}, \\ \mu_{k+1,0} &\leq \frac{1+\varepsilon}{2}\rho_{k,0} + \frac{1-\varepsilon}{2}\mu_{k,0}, \\ \rho_{k+1,0} &= \rho^M(\mu_{k+1,0}). \end{aligned} \tag{25}$$

After straightforward computations, substituting (24) in (25) we have

$$\mu_{k+1,0} \leq \frac{2\varepsilon}{1+3\varepsilon}\mu_k^{\max} + \frac{1+\varepsilon}{1+3\varepsilon}\rho_{k,0} = \mu_3(\rho_{k,0}). \tag{26}$$

From $\rho^* \geq \rho^M(\mu_{k+1,0})$ or $\mu_{k,0} \leq \rho_{k,0}$, it follows that

$$\mu_{k+1,0} \leq -\frac{2\varepsilon}{1-\varepsilon}\mu_k^{\max} + \frac{1+\varepsilon}{1-\varepsilon}\rho_{k,0} = \mu_4(\rho_{k,0}). \tag{27}$$

Notice that $\mu_3(\rho_{k,0}) \geq \mu_4(\rho_{k,0})$ if $\rho_{k,0} \leq \mu_k^{\max}$. Therefore if the latter holds, (26) is fulfilled if (27) is true.

In order to have equilibria configurations, the following relations must hold : $\mu_{k,0} \geq 0$ and $\mu_{k,0} \leq \mu_k^{\max}$. From the condition $\mu_{k,0} \geq 0$, we obtain

$$\rho_{k,0} \geq 2\mu_k^{\max} + \frac{1-\varepsilon}{\varepsilon(1+\varepsilon)}\mu_{k+1,0}$$

which is always true since $\rho_k^{\max} = \frac{2}{1+\varepsilon}\mu_k^{\max}$.

Moreover, from $\mu_{k,0} = \tilde{\mu} \leq \mu_k^{\max}$, it follows that

$$\mu_{k+1,0} \leq \frac{1-2\varepsilon-3\varepsilon^2}{1-\varepsilon}\mu_k^{\max} + \frac{\varepsilon(1+\varepsilon)}{1-\varepsilon}\rho_{k,0} = \mu_5(\rho_{k,0}). \tag{28}$$

Let us analyse two subcases $\alpha_{2.1}) : \rho_{k,0} \geq \mu_k^{\max}$ and $\alpha_{2.2}) : \rho_{k,0} \leq \mu_k^{\max}$.

Case $\alpha_{2.1}$): In this case $\mu_4(\rho_{k,0}) \geq \mu_3(\rho_{k,0})$, therefore the relations (26) and (27) lead to $\mu_{k+1,0} \leq \mu_3(\rho_{k,0})$. Observe that $\mu_3(\rho_{k,0}) \geq \mu_5(\rho_{k,0})$ if

$$(1-\varepsilon-5\varepsilon^2-3\varepsilon^3)\rho_{k,0} \geq (1-\varepsilon-7\varepsilon^2-5\varepsilon^3)\mu_k^{\max},$$

that is always true since $\rho_{k,0} \geq \mu_k^{\max}$. It follows that (26) and (28) are fulfilled if $\mu_{k+1,0} \leq \mu_5(\rho_{k,0})$. Since $\mu_5(\rho_{k,0}) \leq \mu_k^{\max}$ if

$$\frac{1+3\varepsilon}{1+\varepsilon}\mu_k^{\max} \geq \rho_{k,0},$$

it follows that if $\rho_{k,0} \in [\mu_k^{\max}, \frac{1+3\varepsilon}{1+\varepsilon}\mu_k^{\max}]$, then $\mu_{k+1,0} \leq \mu_5(\rho_{k,0})$, and if $\rho_{k,0} \in [\frac{1+3\varepsilon}{1+\varepsilon}\mu_k^{\max}, \rho_k^{\max}]$, then $\mu_{k+1,0} \leq \mu_k^{\max}$.

Case $\alpha_{2.2}$**):** In this case since $\mu_4(\rho_{k,0}) \leq \mu_3(\rho_{k,0})$ the relations (26) and (27) lead to $\mu_{k+1,0} \leq \mu_4(\rho_{k,0})$. From $\mu_{k,0} \leq \rho_{k,0}$ we get

$$\mu_{k+1,0} \leq \frac{2\varepsilon(1+\varepsilon)}{1-\varepsilon}\mu_k^{\max} + \frac{1+\varepsilon}{1-\varepsilon}\rho_{k,0} = \mu_6(\rho_{k,0}). \tag{29}$$

Comparing $\mu_4(\rho_{k,0})$ and $\mu_6(\rho_{k,0})$, it follows that (27) and (29) hold if $\mu_{k+1,0} \leq \mu_6(\rho_{k,0})$. The condition $\mu_6(\rho_{k,0}) \leq \mu_k^{\max}$ is always true, therefore it follows that if $\rho_{k,0} \in [0, \mu_k^{\max}]$ then $\mu_{k+1,0} \leq \mu_6(\rho_{k,0})$.

The equilibria are determined if we fix $\rho_{k,0}$, as it is shown in Figure 9. We notice that the processing rate on the outgoing chain is always less than the value on the incoming one.

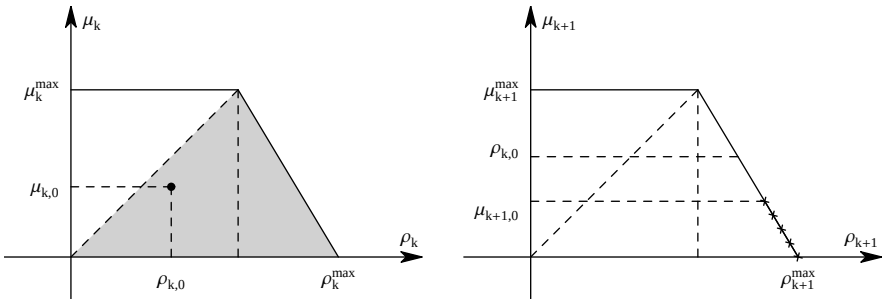

FIGURE 9. Equilibria configurations for the Case α_2).

Case β**):** In this case since $\bar{\mu}_k \leq \mu_{k+1,0}$ we have

$$\mu_{k+1,0} \geq \bar{\mu}_k = \rho_{k+1,0} = \rho_{k,0} = \mu_{k,0}.$$

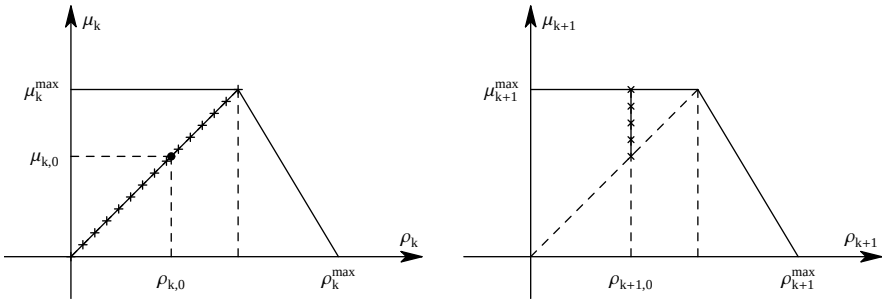

FIGURE 10. Equilibria configurations for the Case β).

Equilibria configurations are depicted in Figure 10. Notice that the two sub-chains have the same density.

5.3. **Riemann Solver SC3.** Let us analyse the case α) and β), outlining only the difference with the equilibria obtained using the Riemann Solver which respects rule SC2.

Case α**):** We have to discuss the subcases $\alpha_1) : \rho^* \leq \rho^M(\mu_{k+1,0})$ and $\alpha_2) : \rho^* > \rho^M(\mu_{k+1,0})$. First we consider case α_1).

Case α_1): We distinguish two cases: $\alpha_{1.1}) : \rho^* > \mu_k^{\max}$ and $\alpha_{1.2}) : \rho^* \leq \mu_k^{\max}$.
Case $\alpha_{1.1}$): The Riemann Solver SC2 and SC3 have the same kinds of equilibria.
Case $\alpha_{1.2}$): In this case, the equilibria are the same: fixed a value $0 \leq \rho_{k,0} \leq \mu_k^{\max}, \mu_{k+1,0}$, and $\rho_{k+1,0} = \rho^*(\rho_{k,0}, \mu_{k+1,0})$ assume values in the same interval individuated for the Riemann Solver SC2. The only difference is that

$$\mu_{k,0} \geq \rho^*(\rho_{k,0}, \mu_{k+1,0}).$$

Case α_2): We have the same kinds of equilibria.
Case β): The equilibria are of the same kind, the only difference is that

$$\mu_{k,0} \geq \rho_{k,0}.$$

5.4. **Equilibria for $\varepsilon = 0$.** We compare the equilibria obtained using the rule SC1, SC2 and SC3, in the case $\varepsilon = 0$. This permits to understand the typical feature of the supply chain at equilibria in the three cases.

$\varepsilon = 0$	SC1	SC2	SC3
α_1)	No equilibria	No equilibria	No equilibria
α_2)	$\mu_{k,0} = \mu_{k+1,0} \leq \rho_{k,0}$, $\rho_{k+1,0} = 2\mu_{k+1}^{\max} - \mu_{k+1,0}$,	Same as SC1	Same as SC1
β)	*either* $\rho_{k,0} = \rho_{k+1,0} \leq \mu_{k,0}, \mu_{k+1,0}$, *or* $\rho_{k+1,0} = \mu_{k,0} \leq \rho_{k,0}$, $\mu_{k+1,0} \geq \frac{1}{2}\rho_{k,0} + \frac{1}{2}\mu_{k,0}$	$\rho_{k,0} = \rho_{k+1,0} = = \mu_{k,0} \leq \mu_{k+1,0}$,	First case of SC1

We first notice that the complicate equilibria of case α_1) disappear from all Riemann solvers.

Regarding case α_2), all rules perform again in the same way. In particular, the processing rates are the same in the entering and exiting lines, while the entering density is greater. To keep the flux equilibrium the exiting density is settled accordingly (the precise value is obtained passing to the limit in $\varepsilon \to 0$).

Let us compare such equilibria with the model of [15], which, for brevity we call GHK model. This case would correspond to a queue which is increasing in size, since the incoming density is bigger than the processing rate. Also to have this situation, we would need $\mu_{k+1,0} = \mu_{k+1}^{max}$. Then we would also have $\rho_{k+1,0} = \mu_{k+1}^{max}$ and the two models well fit.

Finally, we reproduce the situation of an increasing queue, but we may have some equilibria not possible for the GHK model.

Let us now analyse the case β). The first case of SC1 (and thus the only of SC3) corresponds to equal densities, which are lower than the respective processing rates. For the GHK model, this corresponds to an empty queue situation, where the incoming and outgoing fluxes are less than the production rates.

For SC2, we have a quite special case. The incoming density equals the processing rate, while the outgoing density is lower than the corresponding processing rate. Thus again, for the GHK model we have an empty queue situation.

Finally, the second case of SC1 is quite different. In fact, we have the incoming density bigger than the processing rate. While, in the outgoing sub-chain, the density, equal to the incoming one, is definitely below the processing rate. Again, this case corresponds to an empty queue.

Concluding, the model proposed in this paper and that of GHK are comparable for what concerns equilibria. As expected, the emptying queue situation does not appear for the present model, while the choice SC3 seems the more appropriate to reproduce the GHK model features.

6. **Godunov scheme for 2x2 systems.** In order to describe Godunov numerical method as applied to the system (1)- (2), we rewrite it as the 2x2 hyperbolic system (6).

The Godunov scheme is based on the construction of the Riemann problem for (6). The Riemann problem, $[U_L, U_R]$, is the initial value problem for initial data given by a jump discontinuity

$$U(0,x) = \begin{cases} U_L, & x < 0, \\ U_R, & x > 0, \end{cases} \tag{30}$$

and it has a unique entropy solution

$$U(t,x) = U_R\left(\frac{x}{t}; U_L, U_R\right). \tag{31}$$

We discretize $[0,\infty) \times \mathbb{R}$ by a time mesh length Δt and a spatial mesh length Δx and we let $t_n = n\Delta t$ and $x_j = j\Delta x$, so that (t_n, x_j) denotes the mesh points of the approximate solution $v_\Delta(t,x) = v_j^n$. Starting by the approximation $v^n = (v_j^n)_{j\in\mathbf{Z}}$ of $U(t_n,\cdot)$, with v a column vector of $\mathbb{R}^2$, an approximation v_j^{n+1}, with $j \in \mathbb{Z}$, of $U(t_{n+1},\cdot)$ can be defined as follows:

- extension of the sequence v^n as a piecewise constant function $v_\Delta(t_n,\cdot)$:

$$v_\Delta(t_n,\cdot) = v_j^n, \ x_{j-1/2} < x < x_{j+1/2}; \tag{32}$$

- solution of the Cauchy problem

$$\begin{cases} U_t + F(U)_x = 0, \ x \in \mathbb{R}, t > 0, \\ U(0,x) = v_\Delta(t_n,\cdot), \end{cases} \tag{33}$$

  in the cell $(t_n, t_{n+1}) \times (x_{j-1}, x_j)$;
- computation of the solution as the average value of the preceding solution in the interval $(x_{j-1/2}, x_{j+1/2})$ obtained projecting $U(\Delta t,\cdot)$ onto the piecewise constant functions:

$$v_j^{n+1} = \frac{1}{\Delta x}\int_{x_{j-1/2}}^{x_{j+1/2}} U(\Delta t, x)dx. \tag{34}$$

To avoid the interaction of waves in two neighbouring cells before time Δt, we impose a CFL condition like:

$$\frac{\Delta t}{\Delta x} max\{|\lambda_0|, |\lambda_1|\} \le \frac{1}{2}, \tag{35}$$

where λ_0 and λ_1 are the eigenvalues. Since in this case the eigenvalues are such that $|\lambda_0| = 1, |\lambda_1| \le 1$, the CFL condition reads as:

$$\frac{\Delta t}{\Delta x} \le \frac{1}{2}. \tag{36}$$

The solution of (33) is obtained by solving a sequence of neighbouring Riemann problems and we have

$$U(t,x) = U_R\left(\frac{x - x_{j+\frac{1}{2}}}{\Delta t}; v_j^n, v_{j+1}^n\right), \ x_j < x < x_{j+1}, j \in \mathbb{Z}. \tag{37}$$

Then, integrating the equation (33) over the rectangle $(0,\Delta t)\times(x_{j-1/2},x_{j+1/2})$ we can obtain a more explicit expression of the scheme. Since the function is piecewise smooth, we get:

$$\int_{x_{j-\frac{1}{2}}}^{x_{j+\frac{1}{2}}}(U(\Delta t,0)-U(0,x))dx + \int_0^{\Delta t}(F(U(t,x_{j+\frac{1}{2}}-0))-F(U(t,x_{j-\frac{1}{2}}+0)))dt=0. \tag{38}$$

Now, using (32) and projecting the solution on piecewise constant functions we obtain:

$$\Delta x(v_j^{n+1}-v_j^n)+\int_0^{\Delta t}(F(U(t,x_{j+\frac{1}{2}}-0))-F(U(t,x_{j-\frac{1}{2}}+0)))dt=0, \tag{39}$$

and, recalling (37), we derive:

$$v_j^{n+1}=v_j^n-\frac{\Delta t}{\Delta x}\{F(U_R(0-;v_j^n,v_{j+1}^n))-F(U_R(0+;v_{j-1}^n,v_j^n))\}. \tag{40}$$

Since the function $\xi\to F(U_R(\xi;U_L,U_R))$ is continuous at the origin due to the Rankine-Hugoniot conditions (see [14]), Godunov scheme can be written in the form:

$$v_j^{n+1}=v_j^n-\frac{\Delta t}{\Delta x}\{F(U_R(0;v_j^n,v_{j+1}^n))-F(U_R(0;v_{j-1}^n,v_j^n))\}, \tag{41}$$

and the numerical flux computed in $V=(v_1,v_2)$ and $W=(w_1,w_2)$, is

$$G(V,W)=F(U_R(0;V,W)). \tag{42}$$

The numerical flux can be written in a general form as:

$$G(V,W)=\begin{cases}\min_{z_1\in[v_1,w_1]}F(Z) & \text{if } v_1\le w_1,\\ \max_{z_1\in[w_1,v_1]}F(Z) & \text{if } w_1\le v_1,\end{cases}$$

where the second variable z_2 in $Z=(z_1,z_2)$ is assumed to be fixed. The final expression of Godunov scheme for the problem (33) is:

$$v_j^{n+1}=v_j^n-\frac{\Delta t}{\Delta x}\big(G(v_j^n,v_{j+1}^n)-G(v_{j-1}^n,v_j^n)\big). \tag{43}$$

More precisely, for the system (4), the scheme reads as:

$$\begin{cases}\rho_j^{n+1}=\rho_j^n-\frac{\Delta t}{\Delta x}(g(\rho_j^n,\rho_{j+1}^n)-g(\rho_{j-1}^n,\rho_j^n)),\\ \mu_j^{n+1}=\mu_j^n+\frac{\Delta t}{\Delta x}(\mu_{j+1}^n-\mu_j^n),\end{cases} \tag{44}$$

where we indicate the approximate values of $\rho(t,x)$ and $\mu(t,x)$ on the numerical grid as, respectively, ρ_j^n and μ_j^n for $j=0,\dots,L$ and $n=0,\dots,M-1$. Notice that Godunov scheme for the second equation reduces to forward upwind scheme.

6.1. **Approximation algorithm: Fast Godunov for 2x2 systems.** Consider the numerical flux function $F(U)$ with $f(\rho,\mu)$ defined in (4). Since we want to determine a simplified expression for the numerical flux of Godunov scheme, we solve Riemann problems between the two states: (ρ_-,μ_-) on the left and (ρ_+,μ_+) on the right. In particular, referring to relation (42) we compute the value of the flux function F in the separation point between waves of different speeds.

Theorem 17. *The numerical flux function* $G(V,W) = F(U_R(0;V,W))$ *is:*

$$G(\rho_-,\mu_-,\rho_+,\mu_+) = \begin{cases} (\rho_-, -\mu_+) & \text{if } \rho_- < \mu_- \vee \rho_- \le \mu_+, \\ \left(\frac{1-\varepsilon}{1+\varepsilon}\mu_+ + \frac{2\varepsilon}{1+\varepsilon}\rho_-, -\mu_+\right) & \text{if } \rho_- < \mu_- \vee \rho_- > \mu_+, \\ \left(\frac{1+\varepsilon}{2}\rho_- + \frac{1-\varepsilon}{2}\mu_-, -\mu_+\right) & \text{if } \rho_- \ge \mu_- \vee \mu_+ > \tilde{\mu}, \\ \left(\frac{1-\varepsilon}{1+\varepsilon}(\mu_+ + \varepsilon\mu_-) + \varepsilon\rho_-, -\mu_+\right) & \text{if } \rho_- \ge \mu_- \vee \mu_+ \le \tilde{\mu}, \end{cases} \tag{45}$$

with

$$\tilde{\mu} = \mu_- + \frac{1+\varepsilon}{2}(\rho_- - \mu_-). \tag{46}$$

Proof. Let P be the intersection point between the first family curve passing through (ρ_-,μ_-) and the line $\rho = \mu$, namely $P = \begin{pmatrix} \rho_- \\ \rho_- \end{pmatrix}$. The second family curve passing through P splits the invariant region into two regions $A = \{(\rho,\mu) : \mu > \rho_-\}$ (in grey) and $B = \{(\rho,\mu) : \mu \le \rho_-\}$ as depicted in Figures 12 and 13.
Each RP solution presents waves travelling with two velocities, namely $\lambda_0 = -1$ and $0 < \varepsilon \le \lambda_1 \le 1$. Let (ρ_*,μ_*) be the intermediate state, see Fig. 11. We compute the numerical flux function $G(\rho_-,\rho_+)$ given by $(f(\rho_*,\mu_*),\mu_*)$.

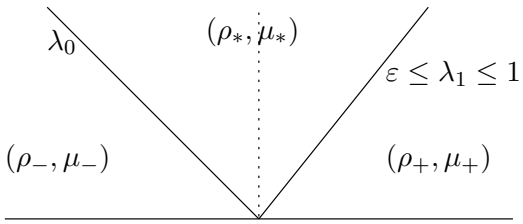

FIGURE 11. Intermediate state between the two waves.

We distinguish two cases

Case 1: $\rho_- < \mu_-$;
Case 2: $\rho_- \ge \mu_-$.

In case 1, if $(\rho_+,\mu_+) \in A$ then $(\rho_*,\mu_*) = (\rho_-,\mu_+)$. Since $\rho_- \le \mu_+$ the flux (3) results to be $f(\rho_-,\mu_+) = \rho_-$.
If $(\rho_+,\mu_+) \in B$, the needed value of flux is that corresponding to $(f(\rho_*,\mu_+),-\mu_+)$, see Fig. 12.

We have:

$$(\rho_*,\mu_*) = (\rho_*,\mu_+) = \begin{pmatrix} \rho_- \\ \rho_- \end{pmatrix} + t\begin{pmatrix} -\frac{1-\varepsilon}{1+\varepsilon} \\ 1 \end{pmatrix}, \tag{47}$$

and ρ_* is computed as:

$$\rho_* = \rho_- + (\rho_- - \mu_+)\frac{1-\varepsilon}{1+\varepsilon}. \tag{48}$$

Finally, since $\rho_* > \rho_- > \mu_+$ we get the expression in the second line of (45). In case 2, if $(\rho_+,\mu_+) \in A$ then $(\rho_*,\mu_*) = (\tilde{\rho},\mu_+)$, where

$$\tilde{\rho} = \frac{1+\varepsilon}{2}\rho_- + \frac{1-\varepsilon}{2}\mu_- \tag{49}$$

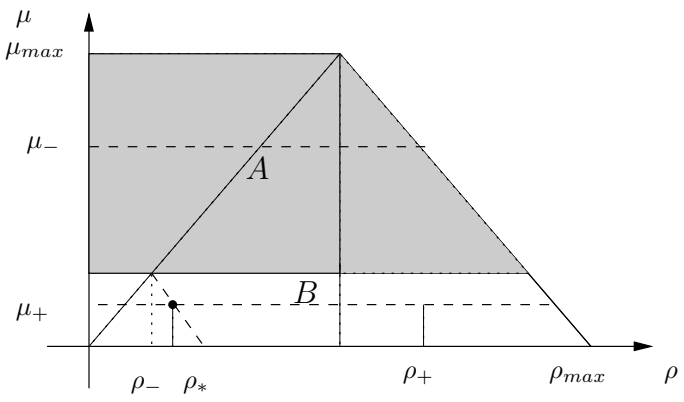

FIGURE 12. Case 1, with $(\rho_+, \mu_+) \in B$.

is obtained as follows. The point $(\tilde{\rho}, \tilde{\mu})$ is:

$$(\tilde{\rho}, \tilde{\mu}) = \begin{pmatrix} \rho_- \\ \mu_- \end{pmatrix} + t \begin{pmatrix} -\frac{1-\varepsilon}{1+\varepsilon} \\ 1 \end{pmatrix},$$

and, using that $\tilde{\rho} = \tilde{\mu}$, one gets (49).

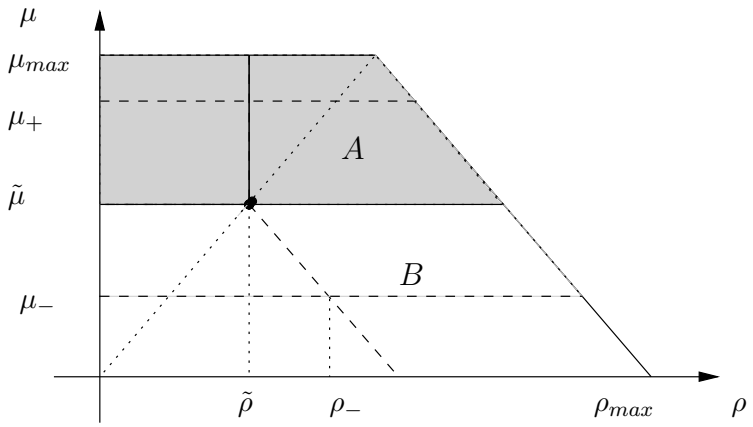

FIGURE 13. Case 2, with $(\rho_+, \mu_+) \in A$.

Assuming $(\rho_+, \mu_+) \in B$, the value of flux we need is $f(\rho_*, \mu_+)$ with ρ_* given by

$$(\rho_*, \mu_*) = (\rho_*, \mu_+) = \begin{pmatrix} \rho_- \\ \mu_- \end{pmatrix} + t \begin{pmatrix} -\frac{1-\varepsilon}{1+\varepsilon} \\ 1 \end{pmatrix}, \tag{50}$$

and, making simple computations, one gets:

$$\rho_* = \rho_- + (\mu_- - \mu_+)\frac{1-\varepsilon}{1+\varepsilon}. \tag{51}$$

Taking into account that $\rho_* > \mu_+$, we obtain the expression of flux as in the last line of (45). □

7. **Numerics for Riemann solvers.** In this Section we describe the numerical framework for the solution of Riemann problems at junctions. In particular, we refer to the general Riemann solver called SC1, already proposed in [10], and to the Riemann solvers introduced here in Section 4, namely SC2 and SC3.
For simplicity, we focus on a single supplier P_k, and on two consecutive sub-chains, namely I_k, I_{k+1}. Let us introduce the notations:

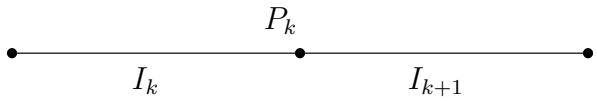

FIGURE 14. Supply chain at a junction.

- $\rho_L^{n,k}, \mu_L^{n,k}$ are the approximate values, respectively, of density and processing rate at time t_n at the outgoing endpoint $x_L = L\Delta x$ of sub-chain I_k;
- $\rho_0^{n,k}, \mu_0^{n,k}$ are the approximate values, respectively, of density and processing rate at time t_n at the incoming endpoint $x_0 = 0$ of sub-chain I_{k+1}.

Let us now describe the discretization of the Riemann solver SC1. If we set

- $\hat{\gamma} = f(\rho_L^{n,k}, \mu_L^{n,k})$,
- $\gamma_{k+1}^{max} = f(\rho_{k+1}^{max}, \mu_0^{n,k+1})$,

we have two cases:

Case *a*) If $\hat{\gamma} \le \gamma_{k+1}^{max}$:

$$\begin{aligned}
\rho_{L+1}^{n,k} &= \rho_L^{n,k},\\
\mu_{L+1}^{n,k} &= \mu_L^{n,k},\\
\rho_{-1}^{n,k+1} &= \begin{cases} f(\rho_L^{n,k}, \mu_L^{n,k}) & \text{if } f(\rho_L^{n,k}, \mu_L^{n,k}) \le \mu_0^{n,k+1},\\ \frac{f(\rho_L^{n,k}, \mu_L^{n,k}) - \mu_0^{n,k+1}}{\varepsilon} + \mu_0^{n,k+1}, & \text{otherwise,} \end{cases}\\
\mu_{-1}^{n,k+1} &= \mu_0^{n,k+1}.
\end{aligned}$$

Case *b*) If $\hat{\gamma} > \gamma_{k+1}^{max}$:

$$\begin{aligned}
\rho_{L+1}^{n,k} &= \rho_L^{n,k},\\
\mu_{L+1}^{n,k} &= \frac{\gamma_{k+1}^{max} - \varepsilon\rho_L^{n,k}}{1-\varepsilon},\\
\rho_{-1}^{n,k+1} &= \rho_{k+1}^{max},\\
\mu_{-1}^{n,k+1} &= \mu_0^{n,k+1}.
\end{aligned}$$

The discretized version of the Riemann solver SC2 is given below.

Case α) We distinguish between the following subcases:

α_1) If $\rho^* < \rho^M$, we set:

$$\begin{aligned}
\rho_{L+1}^{n,k} &= \rho_L^{n,k},\\
\mu_{L+1}^{n,k} &= \min\{\rho^*, \mu_k^{max}\},\\
\rho_{-1}^{n,k+1} &= \rho^*,\\
\mu_{-1}^{n,k+1} &= \mu_0^{n,k+1};
\end{aligned}$$

α_2) if $\rho^* \geq \rho^M$, the new values are:

$$\begin{aligned}
\rho_{L+1}^{n,k} &= \rho_L^{n,k},\\
\mu_{L+1}^{n,k} &= \varepsilon\frac{1+\varepsilon}{1-\varepsilon}\tilde{\rho} - \frac{2\varepsilon}{1-\varepsilon}\bar{\mu}_k + (1+\varepsilon)\mu_0^{n,k+1},\\
\rho_{-1}^{n,k+1} &= \tilde{\rho},\\
\mu_{-1}^{n,k+1} &= \mu_0^{n,k+1};
\end{aligned}$$

Case β)

$$\begin{aligned}
\rho_{L+1}^{n,k} &= \rho_L^{n,k},\\
\mu_{L+1}^{n,k} &= \bar{\mu}_k,\\
\rho_{-1}^{n,k+1} &= \bar{\mu}_k,\\
\mu_{-1}^{n,k+1} &= \mu_0^{n,k+1}.
\end{aligned}$$

The discretization of the Riemann solver SC3 is described in the sequel.

Case α) The following subcases can occur:

α_1) if $\rho^* < \rho^M$, we set:

$$\begin{aligned}
\rho_{L+1}^{n,k} &= \rho_L^{n,k},\\
\mu_{L+1}^{n,k} &= \max\{\rho^*, \mu_L^{n,k}\},\\
\rho_{-1}^{n,k+1} &= \rho^*,\\
\mu_{-1}^{n,k+1} &= \mu_0^{n,k+1};
\end{aligned}$$

α_2) if $\rho^* \geq \rho^M$, we compute the new values as in SC2:

$$\begin{aligned}
\rho_{L+1}^{n,k} &= \rho_L^{n,k},\\
\mu_{L+1}^{n,k} &= \varepsilon\frac{1+\varepsilon}{1-\varepsilon}\tilde{\rho} - \frac{2\varepsilon}{1-\varepsilon}\bar{\mu}_k + (1+\varepsilon)\mu_0^{n,k+1},\\
\rho_{-1}^{n,k+1} &= \tilde{\rho},\\
\mu_{-1}^{n,k+1} &= \mu_0^{n,k+1};
\end{aligned}$$

Case β)

$$\rho_{L+1}^{n,k} = \rho_L^{n,k},$$

β_1) if $\mu_{L+1}^{n,k} \geq \bar{\mu}_k$, we set:

$$\mu_{L+1}^{n,k} = \mu_L^{n,k},$$

β_2) otherwise, we assign:

$$\mu_{L+1}^{n,k} = \bar{\mu}_k,$$

$$\rho_{-1}^{n,k+1} = \bar{\mu}_k,$$
$$\mu_{-1}^{n,k+1} = \mu_0^{n,k+1}.$$

8. **Numerical tests.** As an application of the supply chain dynamics presented in Sections 2-4 and the associated numerical algorithm described in Section 6, we present some experiments on sample cases. The problem (4) is discretized using Godunov and Upwind schemes, as indicated in (44), with the numerical flux (45). We set space increment equal on each supplier, namely $N_k = \frac{L_k}{\Delta x}$, where N_k is the number of space discretization points. The time steps Δt are constants and are obtained imposing the CFL condition on each arc.

In the following Tests 1 and 2 we refer to numerical examples presented in the papers by Klar and coauthors, [15, 16], in such a way to establish a comparison between their and our approach. To this aim we consider the flux function with different slopes (5). The expression of numerical flux $G(\rho_-, \mu_-, \rho_+, \mu_+)$ of Fast Godunov scheme for supplier I_k is:

$$G = \begin{cases} (m_k \rho_-, -\mu_+) & \text{if } \rho_- < \mu_- \vee \rho_- \leq \mu_+, \\ \left(\left(m_k - \frac{2\varepsilon}{1+\varepsilon}\right)\mu_+ + \frac{2\varepsilon}{1+\varepsilon}\rho_-, -\mu_+\right) & \text{if } \rho_- < \mu_- \vee \rho_- > \mu_+, \\ \left(m_k\left(\frac{1+\varepsilon}{2}\rho_- + \frac{1-\varepsilon}{2}\mu_-\right), -\mu_+\right) & \text{if } \rho_- \geq \mu_- \vee \mu_+ > \tilde{\mu}, \\ \left(\left(m_k - \frac{2\varepsilon}{1+\varepsilon}\right)\mu_+ + \frac{\varepsilon(1-\varepsilon)}{1+\varepsilon}\mu_- + \varepsilon\rho_-, -\mu_+\right) & \text{if } \rho_- \geq \mu_- \vee \mu_+ \leq \tilde{\mu}, \end{cases} \tag{52}$$

with $\tilde{\mu}$ as in (46).

8.0.1. *Test 1.* As in [15], we consider a supply chain network consisting of $N = 4$ suppliers and we use the data in Table 1.

Processor k	μ_k	m_k	L_k
1	25	1	1
2	15	0.2	0.2
3	10	0.2	0.6
4	15	0.2	0.2

TABLE 1. Parameters of the test problem 1.

Let us assume the following initial and boundary data:

$$\rho_1(0,x) = \rho_2(0,x) = \rho_3(0,x) = \rho_4(0,x) = 0, \tag{53}$$

$$\rho_1(t,0) = \begin{cases} \frac{18}{35}t, \text{ if } 0 \le t \le 35, \\ -\frac{18}{35}t + 36, \text{ if } 35 < t \le 70, \\ 0, \text{ if } t > 70, \end{cases}$$

and the space and time intervals are, respectively, $[0,2]$ and $[0,140]$, with $\Delta x = 0.02$ and $\Delta t = 0.01$. On each processor $k = 1,2,3,4$ we assume as the initial datum $\mu(0,x)$ the value μ_k, which is also imposed at the incoming and outgoing boundaries. Notice that the inflow profile $\rho_1(t,0)$ is assigned on the first processor, which can be considered as an artificial arc, and it exceeds the maximum capacity of the other processors.

In Fig. 15 it is depicted the evolution in time on processors 2, 3, 4, of flux, density and processing rate, obtained by the Riemann solver SC1 for $\varepsilon = 0.1$.

From the analysis of graphics in Fig. 15, we can deduce that the processing rate, according to SC1, is minimized and, consequently, the flux and the density are considerably lowered and are almost plateau shaped on processors 3 and 4. On the other hand, SC2 determines the behaviour showed in Fig. 16, where the flux and the density are correctly developed on processors 2, 3, 4, due to the behaviour of the processing rate depicted in the graphics, which assumes the minimum possible value in order to maximize the flux.

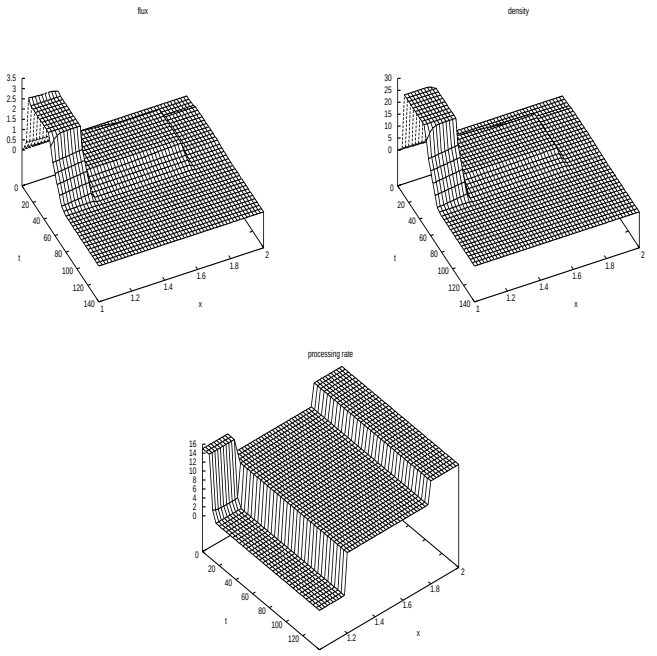

FIGURE 15. Test 1: evolution on processors 2, 3, 4, of f (top left), ρ (top right) and μ (bottom) using SC1, with data in Table 1 and $\varepsilon = 0.1$.

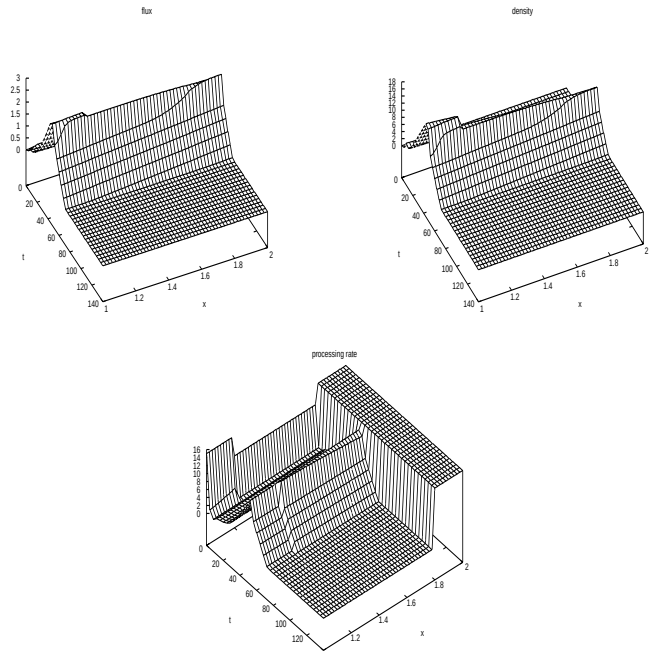

FIGURE 16. Test 1: evolution on processors 2, 3, 4, of f (top left), ρ (top right) and μ (bottom) using SC2, with data in Table 1 and $\varepsilon = 0.1$.

In the following Fig. 17, 18 and 19 it is depicted the evolution in time on processors 2, 3, 4, of flux, density and processing rate, as obtained by the Riemann solver SC3 with, respectively, $\varepsilon = 0.1$, $\varepsilon = 0.5$ and $\varepsilon = 0.01$. As showed by the graphics obtained, ε varying determines a different evolution. In particular, for ε tending to zero, the maximum values assumed by the flux and the density decrease.

From the analysis of graphics in Figg. 17, 18 and 19, obtained by applying Riemann solver SC3, we can deduce that adjustments of processing rate determine the expected behaviour of the density, also in accordance with results reported in [15].

8.0.2. *Test 2.* Referring to [16], we consider again a supply chain of $N = 4$ suppliers and impose the following initial and boundary data:

$$\begin{aligned} &\rho_1(0,x) = \rho_2(0,x) = \rho_3(0,x) = \rho_4(0,x) = 0, \\ &\rho_1(t,0) = \frac{\mu_2}{2}(1 + \sin(3\pi t/T_{max})), \end{aligned} \tag{54}$$

where the space interval is $[0,6]$ and the observation time is $T_{max} = 20$, with $\Delta x = 0.1$ and $\Delta t = 0.05$. On each processor $k = 1,2,3,4$ we assume $\mu(0,x) = \mu_k$ and incoming and outgoing boundary data are given by μ_k. Observe that even in this case the inflow profile $\rho_1(t,0)$ exceeds the maximum capacity of the processors. Referring to [16] we make simulations setting parameters as in Table 2 and we

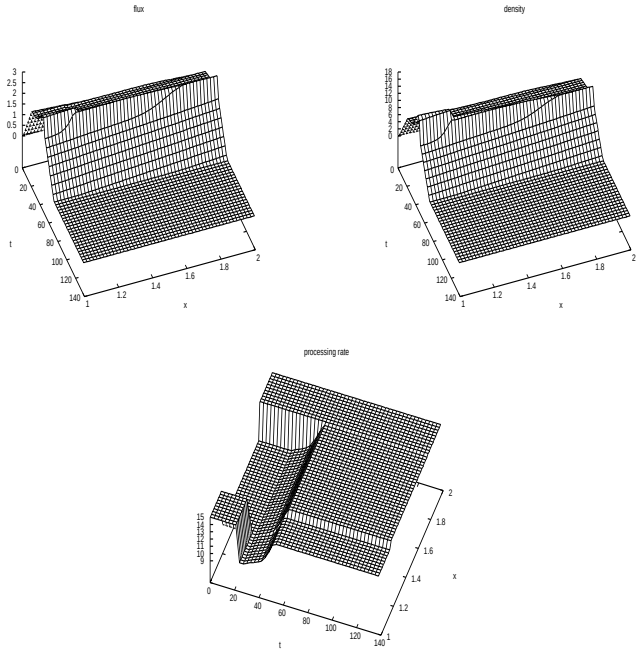

FIGURE 17. Test 1: evolution on processors 2, 3, 4, of f (top left), ρ (top right) and μ (bottom) using SC3, with data in Table 1 and $\varepsilon = 0.1$.

assume to have default processing velocities on each processor, namely $m_k = 1, k = 1, 2, 3, 4$.

Processor k	μ_k	L_k
1	99	1
2	15	1
3	10	3
4	8	1

TABLE 2. Parameters of the test problem 2.

In the next Fig. 20 it is depicted the evolution in time of density and processing rate obtained by the Riemann solver SC1 for $\varepsilon = 0.1$, while in Figg. 21 and 22 we show the behaviour of flux, density and processing rate obtained, respectively, by the Riemann solver SC2 and SC3.

Let us make a comparison between graphics in Figg. 20 and 21. We observe that with solver SC2 the productivity collapses, thus provoking a lowering in the values of the flux and the density. On the other hand, SC1 maintains the level of productivity. Using solver SC3, which maximizes the flux and adjusts the processing rate if necessary, results are in accordance with those obtained in [16], see Fig. 22.

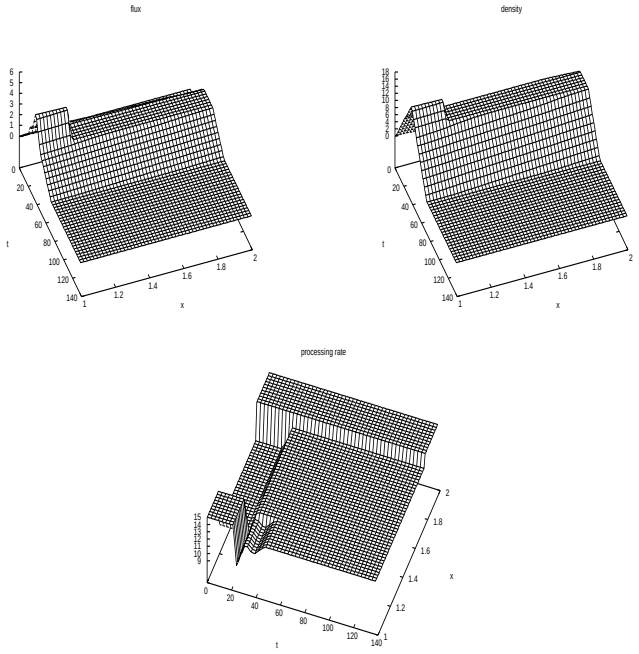

FIGURE 18. Test 1: evolution on processors 2, 3, 4, of f (top left), ρ (top right) and μ (bottom) using SC3, with data in Table 1 and $\varepsilon = 0.5$.

8.1. **CPU time.** Now we are interested in the analysis of the CPU time. In particular, we want to compare the performances of programs based on the classical Godunov scheme (G) and on the Fast Godunov scheme (FG) introduced in Section 6.1. To this aim, we report in the following Tables 3 and 4 the time of execution, expressed in seconds (s), of the simulation algorithm using SC3 and applied, respectively, to Test 1 and to Test 2, when Δx (and consequently $\Delta t = \Delta x/2$), decreases.

In order to show the complexity, depending on the number of nodes as well as the space-time discretizations, of the simulation algorithm characterized by the proposed Riemann solvers, we consider networks composed large number of nodes. In the following table 5 we display the CPU time expressed in seconds of the simulation algorithm using SC3 applied to supply chains of $N = 100, 1000, 10000$ suppliers.

From the analysis of the previous tables we can observe that the Fast Godunov scheme (FG) allows to save more than 40% of CPU time with respect to the classical Godunov scheme G. Therefore we can conclude that FG performs better than G. We point out that the growth in the CPU time due to the increasing dimension of supply chain seems to be quadratic.
All the simulations have been performed by a personal computer, processor AMD Athlon XP 2400 Mhz, RAM 512 Mb.

9. **Conclusions.** In this paper we extended the model for supply chain dynamics of [10], based on a system of conservation laws, one for the part density and the

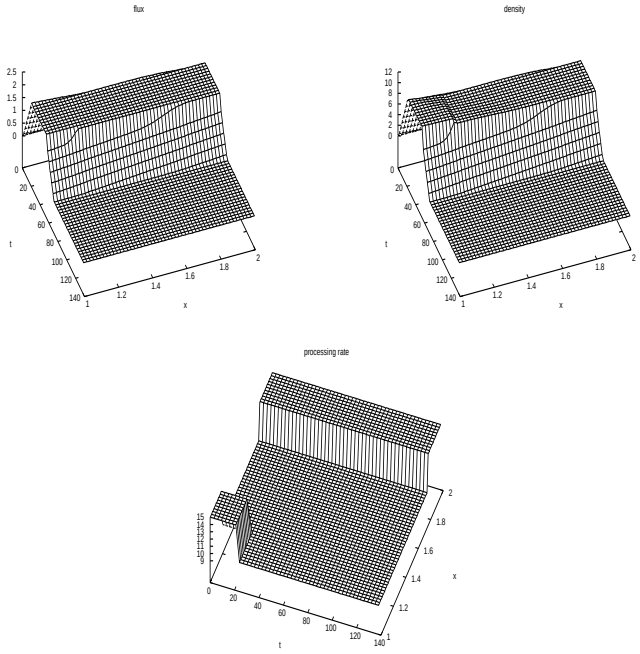

FIGURE 19. Test 1: evolution on processors 2, 3, 4, of f (top left), ρ (top right) and μ (bottom) using SC3, with data in Table 1 and $\varepsilon = 0.01$.

CPU time		
	$T = 140$	
Δx	G	FG
0.1	0.06 s	0.04 s
0.05	0.19 s	0.12 s
0.025	0.71 s	0.4 s
0.0125	2.81 s	1.57 s
0.00625	13.5 s	7.0 s

TABLE 3. CPU time for the schemes G and FG applied to Test 1, $T = 140$.

other for the processing rate. We proposed some alternative definitions for solutions at nodes: maximizing the flux with possible adjustments of the processing rate.

For the newly obtained dynamics, we compute the set of equilibria and compare them with the model of [15], consisting of a single conservation law for densities and odes for queues' buffer occupancies.

Then we provide a fast Godunov scheme for solutions of numerical problems. The obtained results show that the choice of maximizing the flux, while minimizing the changes in the processing rate, gives rise to the most interesting dynamics, which

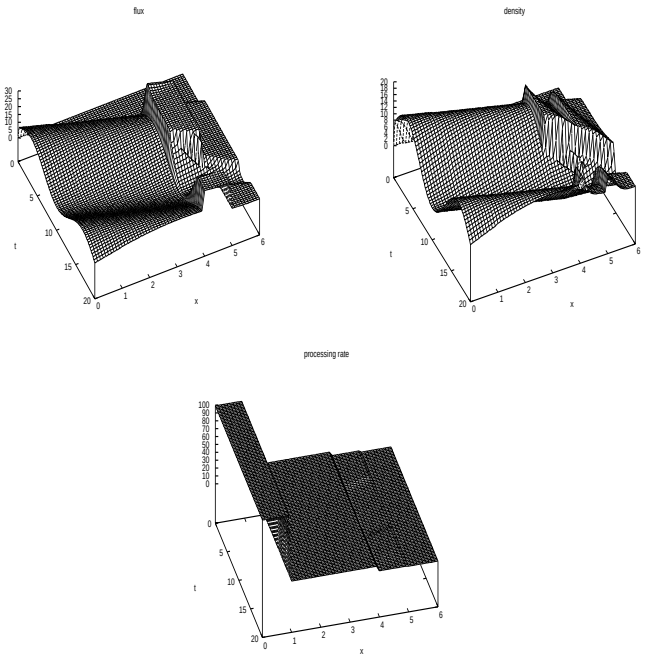

FIGURE 20. Test 2: evolution of f (top left), ρ (top right), μ (bottom) for the default velocities using SC1, with data in Table 2 and $\varepsilon = 0.1$.

CPU time		
	$T = 20$	
Δx	G	FG
0.2	0.01 s	0.01 s
0.1	0.02 s	0.02 s
0.05	0.07 s	0.04 s
0.025	0.25 s	0.16 s
0.0125	1.0 s	0.6 s

TABLE 4. CPU time for the schemes G and FG applied to Test 2, $T = 20$.

also fits better with the model of [15]. Such results are confirmed by numerical tests taken from [15, 16].

REFERENCES

[1] D. Armbruster, P. Degond and C. Ringhofer, *A model for the dynamics of large queuing networks and supply chains*, SIAM J. Appl. Math.**66** (2006), 896-920.

[2] D. Armbruster, P. Degond and C. Ringhofer, *Kinetic and fluid models for supply chains supporting policy attributes*, Bull. Inst. Math. Acad. Sin. (N.S.) **2** (2007), no. 2, 433-460.

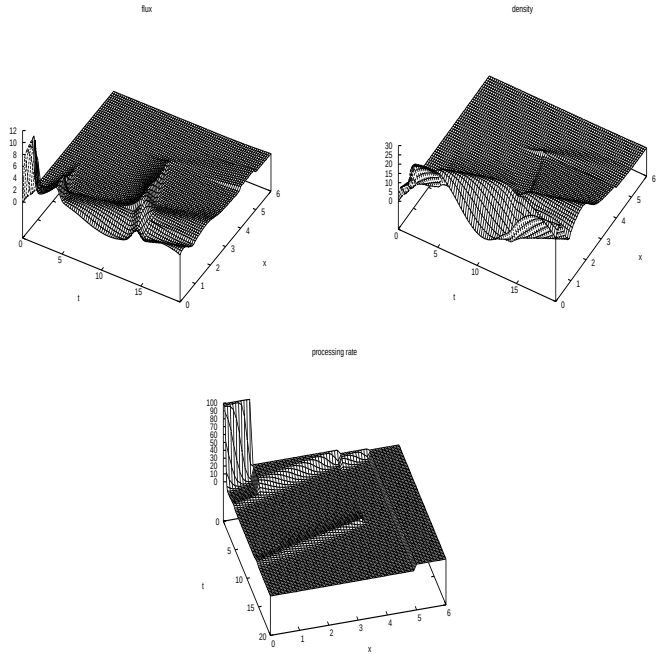

FIGURE 21. Test 2: evolution of f (top left), ρ (top right), μ (bottom) using SC2, with data in Table 2 and $\varepsilon = 0.1$.

CPU time						
$T = 140$						
	$N = 100$		$N = 1000$		$N = 10000$	
Δx	G	FG	G	FG	G	FG
0.1	3.4 s	2.9 s	314.2 s	272.6 s	30981.9 s	26816.2 s
0.05	7.5 s	6.8 s	603.2 s	525.5 s	59629.1 s	51088 s
0.025	19 s	16.2 s	1422.9 s	1208.7 s	138310.7 s	117502.4 s
0.0125	57.2 s	44.1 s	3558 s	2900.6 s	365281.5 s	282005.8 s
0.00625	202.3 s	138.9 s	10010.9 s	7832.2 s	1059316.3 s	761415.7 s

TABLE 5. CPU time of the algorithm for the schemes G and FG, for $T = 140$ and $N = 100, 1000, 10000$.

[3] D. Armbruster, D. Marthaler and C. Ringhofer, *Kinetic and fluid models hierarchies for supply chains*, SIAM J. on Multiscale Modeling and Simulation, **2** (2003), 43-61.
[4] M. Banda, M. Herty and A. Klar, *Gas flow in pipeline networks*, Networks and Heterogeneous Media, **1** (2006), 41–56.
[5] A. Bressan, "Hyperbolic Systems of Conservation Laws - The One-dimensional Cauchy Problem",Oxford Univ. Press, 2000.
[6] Y. Chitour and B. Piccoli, *Traffic circles and timing of traffic lights for cars flow*, Discrete and Continuous Dynamical Systems-Series B, **5** (2005), 599–630.
[7] G. Coclite, M. Garavello and B. Piccoli, *Traffic flow on road networks*, SIAM J. Math. An., **36** (2005), 1862-1886.

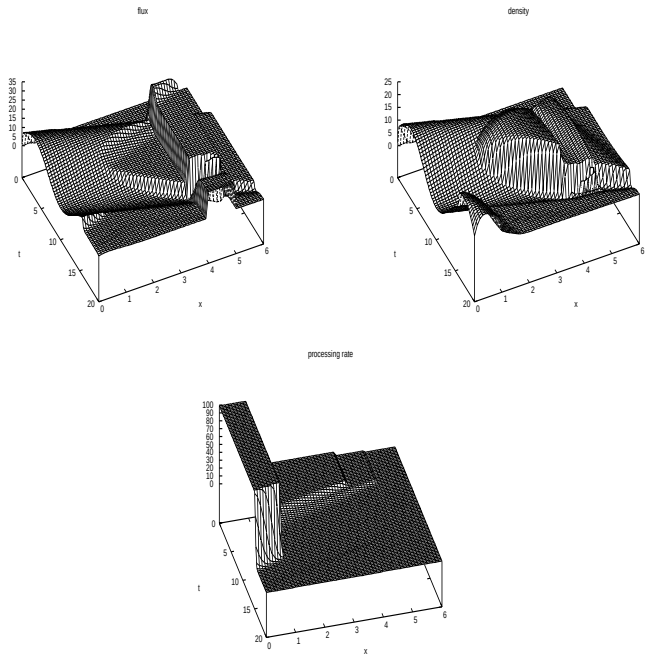

FIGURE 22. Test 2: evolution of f (top left), ρ (top right), μ (bottom) using SC3, with data in Table 2 and $\varepsilon = 0.1$.

[8] C. Dafermos, "Hyperbolic conservation laws in Continuum physics" Second edition.[Fundamental Principles of Mathematical Sciences], 325, Springer-Verlag, Berlin, 2005.
[9] C. F. Daganzo, "A theory of supply chains", Lecture notes in Economics and Mathematical Systems, 526, Springer Verlag, New York, Berlin, Heidelberg, 2003.
[10] C. D'Apice and R. Manzo, *A fluid-dynamic model for supply chain*, Networks and Heterogeneous Media (NHM), **1** (2006), 379-398.
[11] C. D'Apice, R. Manzo and B, Piccoli, *Packets flow on telecommunication networks*, SIAM Journal of Mathematical Analysis **38** (2006), 717–740.
[12] M. Garavello and B. Piccoli, *Source destination flow on a road network*, Comm. Math. Sci., **3** (2005), 261-283.
[13] M. Garavello and B. Piccoli, *Traffic flow on a road network using the Aw-Rascle model*, Comm. on PDE **31** (2006), 243–275.
[14] E. Godlewski and P. A. Raviart,"Hyperbolic Systems of Conservation Laws", Mathématiques & Applications [Mathematics and Applications], 3/4. Ellipses, Paris, (1991).
[15] S. Göttlich, M. Herty and A. Klar,*Network models for supply chains*, Comm. Math. Sci, **3** (2005), 545-559.
[16] S. Göttlich, M. Herty and A. Klar, *Modelling and optimization of supply chains on complex networks*, Comm. Math. Sci., **4** (2006), 315–330.
[17] D. Helbing, S. Lämmer, T. Seidel, P. Seba and T. Platkowski, *Physics, stability and dynamics of supply networks*, Physical Review E, **70** (2004).
[18] D. Helbing and S. Lämmer, *Supply and production networks: From the bullwhip effect to business cycles*, in "D. Armbruster, A. S. Mikhailov, and K. Kaneko (eds.) Networks of Interacting Machines: Production Organization in Complex Industrial Systems and Biological Cells", World Scientific, Singapore, 2005, 33-66.
[19] M. Herty and A. Klar, *Modeling, simulation, and optimization of traffic flow networks*, SIAM J. Sci. Comput., **25** (2003), 1066–1087.
[20] M. Herty, A. Klar and B. Piccoli, *Existence of Solutions for Supply Chains Models Based on Partial Differential Equations*, SIAM J. Math. Anal., **39** (2007), 160–173.

[21] H. Holden and N.H. Risebro, *A mathematical model of traffic flow on a network of unidirectional roads*, SIAM J. Math. Anal., **26** (1995), 999–1017.
[22] J.P. Lebacque, *The Godunov scheme and what it means for first order flow models*, in "Transportation and Traffic Theory, Proceedings of the 13th ISTTT (J.B. Lesort ed.)", 1996, Pergamon, Oxford, 647-677.
[23] M. J. Lighthill and G. B. Whitham, *On kinetic waves. II. Theory of traffic flows on long crowded roads*, Proc. Roy. Soc. London Ser. A, **229** (1955), 317-345.
[24] P. I. Richards, *Shock Waves on the Highway*, Oper. Res., **4** (1956), 42-51.

Received April, 2007; revised August 2007.

E-mail address: g.bretti@iac.cnr.it
E-mail address: dapice@diima.unisa.it
E-mail address: manzo@diima.unisa.it
E-mail address: b.piccoli@iac.cnr.it